A PERMANENT-MAGNET OSCILLATING GENERATOR

By

WARREN E. RAY

Bachelor of Science

Oklahoma Agricultural and Mechanical College

Stillwater, Oklahoma

1952

Submitted to the faculty of the Graduate School
of the Oklahoma Agricultural and Mechanical
College in partial fulfillment of the
requirements for the degree of
MASTER OF SCIENCE
August, 1956

A PERMANENT-MAGNET OSCILLATING GENERATOR

Paul A. McCollum
Thesis Adviser

C. Nader
Faculty Representative

Robert MacVicar
Dean of the Graduate School

PREFACE

This thesis reports the work performed on the design, material selection and procurement, fabrication, investigation, test, and analysis of the performance of a PERMANENT-MAGNET OSCILLATING GENERATOR representing a portion of the research requirement under a contract with the Wright Air Development Center, U.S. Air Force, covering the investigation of unconventional power supplies. The basic principle involved is that of production of a voltage by vibrating a coil in a magnetic field supplied by a permanent magnet.

The design and development of a new product is both slow and expensive. This work and thesis were made possible only with the financial resources afforded under the above-mentioned contract.

I wish to thank Professor Paul A. McCollum, P.E., for his guidance in the capacity of adviser and as project leader.

Thanks are also extended to Professor L. J. Fila for the design of the mechanical shaker, to Mr. Ralph Fisher for the design and construction of the strain gage amplifier and for invaluable help in the performance tests, and finally to Mr. Tom Ewing for aiding with the performance tests.

The writer wishes to thank the machinists in the Research and Development Laboratory of the Oklahoma Institute of Technology for the production of components with unusual requirements. These men are: Mr. P. G. Wilson, Mr. R. Anderson, Mr. E. L. Deshazo, and Mr. A. L. Harris.

Finally, the writer appreciates the fine work of Mr. K. G. Hoffer of the Oklahoma Institute of Technology Duplicating Service.

TABLE OF CONTENTS

LIST OF FIGURES

LIST OF PLATES

CHAPTER I

INTRODUCTION

To the electrical engineer parts of this thesis will be of such fundamental nature as to appear superfluous or unnecessary. However, at the request of the Air Force, full explanation and development will be employed throughout since it is by no means certain that only technically trained personnel will peruse these pages.

Aside from a historical review the material falls naturally into background theory, preliminary model and tests, optimum permanent-magnet assembly design, coil and coil frame design, design of the driving power source with methods of measuring force input, power output, frequency, displacement, and other items as may be desirable, performance tests, analysis of results, and overall conclusions. Accordingly, these items will be discussed in the following chapters in the order named.

Some work along these lines was done by John Barton, Jr., Master of Science, Oklahoma A&M College, August, 1955, and reported in a thesis entitled "An Oscillating Electric Generator." However, a d.c. exciting coil was used instead of a permanent magnet, and the highest frequency used was twenty cycles per second (cps). It is now desired to use a design frequency of 400 cps with tests to be made from a low frequency to 1000 cps if possible. A coil displacement of one-tenth of an inch was tentatively selected. However, objects do not easily vibrate at 1000 cps with the displacement selected without breaking, due to the high

accelerations involved, even with weights made as small as possible. Since this problem appeared to be tremendous, a mechanical engineer was engaged to design a mechanical shaker. An electrodynamic shaker, if available, might be used to advantage.

A word on units seems appropriate. Modern texts in the electrical field use the rationalized meter-kilogram-second (MKS) system of units. The writer is in agreement with this trend. However, permanent magnet manufacturers still use the centimeter-gram-second (CGS) system of units in their literature. Moreover, the permeability of air and of nonmagnetic material is unity. Most physical measurements in this work are small. Therefore, for reasons cited above, the CGS system will be used in parts of this work. Where other systems are used, the change-over will be developed.

CHAPTER II

HISTORICAL REVIEW

Discovery of the lodestone (leading stone), a natural magnet of iron oxide, Fe_3O_4, sometimes called magnetite, dates back some 3000 years. The ore was abundant in Magnesia, a province in ancient Greece. The word "magnet" probably was derived from the name of the province. However, another tradition states that the term owes its origin to Magnes, a Greek shepherd, who discovered a piece of ore clinging to the end of his iron-shod crook while tending his flocks in Asia Minor. The magnetized iron on the crook is known as an artificial magnet. Somewhat astounding is the fact that the lodestone lost none of its magnetic properties in magnetizing the piece of iron. Perhaps this is an exception to the rule that one may not obtain something for nothing.

About the twelfth century it was discovered that a magnet suspended in the middle would rotate until its ends pointed north and south. If the north-seeking end of the magnet is called a magnetic north pole, then evidently the geographical North pole contains a south magnetic pole since unlike poles attract. In any event, without the magnetic compass, Columbus might not have made so much history.

Old records indicate that around 600 B.C. the ancients were aware that amber and jet rubbed with silk had the power to attract pieces of straw, leaves, and feathers. The word "electricity" comes from the Latin electrum, meaning amber.

Gilbert, an English physician, published some observed magnetic phenomena in 1600, laying the foundation for what was to come. In 1820, Hans Christian Oersted (University of Copenhagen, Denmark) made the momentous discovery that there was a connection between electricity and magnetism. He demonstrated that when an electric current is passed through a wire near a compass, the needle tends to turn at right angles to the wire. Then Andre Marie Ampere, a Frenchman, found that two wires carrying electrical current act toward each other exactly like magnets. Sir Humphry Davy, an Englishman, demonstrated that pieces of iron could be magnetized if placed near a current-carrying conductor. In 1825, William Sturgeon invented the electromagnet by winding a copper wire around an iron bar. In 1831, another Englishman, Michael Faraday, the son of a poor blacksmith, showed that when a coil of wire is cut by magnetic flux a voltage was produced in the coil. Motion of the magnet was the means by which mechanical power was changed to electricity. None of the magnetism was used, that is, magnetic energy was not changed to electrical energy. To this day no one knows why there should be a voltage generated when the magnetic flux linking a coil undergoes a change.

The invention of the self-exciting dynamo in 1865 ushered in the era of electricity--the beginning of our modern electrical age.

The modern magnet, magnetized by electromagnetic methods, evolved from Oersted's discovery. However, the materials for magnets lagged, primarily because metallurgists were not interested in the magnetic properties of metals. Most permanent magnet materials originated as tool steels. In 1917, impetus was given to the search for better materials by the Japanese (Honda and Takei) discovery of the magnetic properties of cobalt magnet steel. Since this date, attention was given to developing

certain materials primarily for their magnetic properties.

Two distinct classes of magnetic materials are recognized today. If a member of the first group is placed in the path of an external magnetic field, the field is concentrated. As soon as the external force is removed, however, the field collapses and the material returns essentially to the same state as before it was magnetized. The materials in this group are magnetically "soft." Material of the second group differs in that when a magnetic field is removed the alloy retains a portion of the magnetism, and therefore becomes a permanent magnet. These materials are considered magnetically "hard," and are known as "Permanent Magnet Materials."

The development of permanent magnet materials progressed with the major contribution again being made by the Japanese, Mishima, in 1932, with the announcement of the Nickel-Iron-Aluminum alloys. A further improvement was made by Horsburgh and Tetly in 1934 with the addition of cobalt and copper. The new material was known as "ALNICO," which is in use today, with many variations, as will be shown later.

There are many other magnetic materials (some again originating in Japan) in use today, but this thesis will be focused upon Alnico.

CHAPTER III

FUNDAMENTAL THEORY

A. INDUCED VOLTAGE[1]

Experimental evidence shows that an induced voltage is

$$e = d\Phi/dt\ 10^{-8} \text{ volts} \qquad (1)$$

where Φ is the flux linkages (lines of flux times number of turns linked) and t is in seconds. This is known as Faraday's Law.

Place a coil of N turns and A square centimeters of area in a magnetic field of B lines per square centimeter so that the plane of the coil is perpendicular to the lines of the magnetic field. Let the total flux, ϕ, enclosed by the coil be, $\phi = AB$. Then $\Phi = NAB$. By equation (1),

$$e = d/dt\ (NAB)10^{-8} \text{ volts} = N(B\ dA/dt + A\ dB/dt)10^{-8} \text{ volts.} \qquad (2)$$

If the area of the coil does not vary with time, equation (2) reduces to the "transformer equation":

$$e = NA\ dB/dt\ 10^{-8} \text{ volts.} \qquad (3)$$

When the flux density is constant, equation (2) reduces to

$$e = NB\ dA/dt\ 10^{-8} \text{ volts.} \qquad (4)$$

The coil area need not physically change because an equivalent condition prevails when the projection of the coil area upon a plane area perpendicular to the magnetic field presents a changing area. An example would be

---

[1] Applications Course, (General Electric Company, Schenectady, 1947), p. 3.

a revolving coil in a magnetic field.

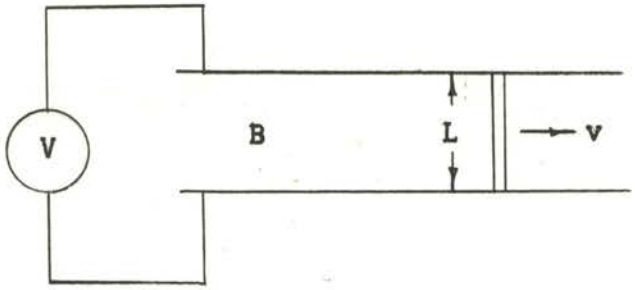

Figure 1

In Figure 1, consider the shorting bar of length L, moving at a velocity v across a constant field of B lines per square unit of area. When B, L, and v are not mutually perpendicular, use should be made of mutually perpendicular components, since only these are effective in producing a voltage. For a constant B, dA/dt becomes Lv, and equation (4) may be written as

$$e = NBLv \text{ abvolts} = NBLv10^{-8} \text{ volts.} \qquad (5)$$

The energy comes from mechanical energy supplied and not from B. This is the familiar "speed voltage" equation. When B is not a constant, equation (2), as rewritten below, must be used.

$$e = N(BLv + A\, dB/dt)10^{-8} \text{ volts.} \qquad (6)$$

Any consistent unit of length may be used since length to the second power appears in both the numerator and denominator. The ultimate quantity is in the units of lines per second. In this work, B is in lines per square centimeter or gausses, L is in centimeters, v is in centimeters per second (may be in the form of an equation), and N is in turns. The direction of each term of equation (6) may be determined by Lenz's Law which states: "The emf induced in a circuit by a change in flux will be in the direction current WOULD have to flow in order to oppose the CHANGE in flux." This is a statement of the law of conservation of energy in electrical terms.

The word, CHANGE, is capitalized to emphasize that it is the change in flux to be opposed, and not the flux. WOULD is also capitalized to show that the voltage is induced whether or not the circuit is closed so that current flows. With hazard to life, one may prove this by grasping in either hand the open-circuited terminals of a transformer secondary or the output terminals of a generator. As a matter of interest, a voltage would be induced in any nonconducting material such as glass or wood used as the sliding bar in Figure 1 even though current would not flow because of a scarcity of free electrons.

> Numerous paradoxical circuits and arrangements can be devised in which an emf might be predicted by one of the rules and experiment prove the emf non-existent, or on the other hand no emf might be predicted and experiment prove one to exist.[2]

It follows that theory should be checked with laboratory experiment.

Carl Hering,[3] in 1908, evoked considerable comment from the electrical giants of the era such as Charles P. Steinmetz, A. E. Kennelly, Elihu Thomson, and others.[4]

> The object of this paper is to point out that the usual and well-known statement of the fundamental law of induction of currents by magnetic flux is not correct as a universal law, and requires to be modified; when, applied as it is usually stated, it sometimes gives entirely erroneous results, although it is correct under the usual conditions. An essential qualification has apparently been overlooked. The proof is given by a simple experiment.

Other writers merely used different expression to the same

---

[2]Robert P. Ward, Introduction to Electrical Engineering, (2d. ed., New York, 1952), p. 252.

[3]Carl Hering, "An Imperfection in the Usual Statement of the Fundamental Law of Electromagnetic Induction." Proceedings of the American Institute of Electrical Engineers, Vol. 27, Part 1, (New York, 1908), p. 339.

[4]Proceedings of the American Institute of Electrical Engineers, Vol. 27, Part 2, (New York, 1908), pp. 1362-1370.

> effect. One well-known form of expressing this law is to consider the magnetic circuit and the electric circuit to be like two links of a chain: then, during the process of linking them together, an emf is induced in one direction; when unlinking them an exactly equal emf is induced in the other direction.

Mr. Hering's Figure one contains a horseshoe magnet, a metallic spring clip very much like an enlarged spring-type clothes pin so that the clip may either be pulled off of a leg of the magnet or removed perpendicularly to a leg with the clip arms always in contact with the magnet leg so that the electrical circuit is not broken. Copper wires attached to the clip ends connect to a current galvanometer.

> In moving the clip over the end of the horseshoe magnet a current flowed in the circuit. The magnetic flux has thereby been linked with the electric circuit; the flux enclosed by the circuit has been increased from zero to the maximum; or to use Faraday's terms, the lines of force in the air from one pole to the other have been cut by the conductor. So far, the law as it is stated, is correct.
>
> If this loop be moved as shown [Hering's figure] from the dotted position to the one shown in full by passing the leg of the magnet through the joint of the loop [i.e., the electric circuit], but WITHOUT OPENING the circuit, the flux and the circuit will be unlinked again. . . . . .
>
> According to the law of induction as quoted from Maxwell or J. J. Thomson, and as almost universally accepted, there ought then to be an emf induced . . . . . The fact is, however, quite the contrary; there is absolutely no emf induced by this unlinking.
>
> The conclusion reached was that it is NOT the linking and unlinking of the magnetic and the closed electric circuits, NOT the changing of the amount of flux enclosed in the closed circuit, but that it is the MATERIAL OF THE CONDUCTOR OF THE CURRENT, and not merely the circuit itself, which must actually move across the flux (or the flux move across it) in order to cause induction.

This experiment was witnessed by Dr. Northrup of Leeds & Northrup Company.

B. FORCE ON A CURRENT-CARRYING CONDUCTOR IN A MAGNETIC FIELD.

Experiments performed by Ampere about 1824 show that the electromagnetic force that acts between very long current-carrying conductors

which lie parallel obeys the equation[5]

$$F = \mu L I_1 I_2/(2\pi S) \tag{7}$$

where F is the force in dynes, μ is the permeability of the medium surrounding the wires, L is the parallel length of the conductors in centimeters, I_1 and I_2 are the currents in the conductors in abamperes (1 abampere = 10 amperes), and S is the separation of the conductors in centimeters.

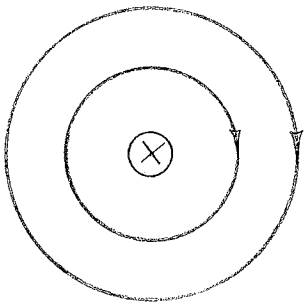

Figure 2. Magnetic field surrounding a long, straight conductor.

With the right hand grasping a conductor with the thumb in the current direction (as in Figure 2) Ampere's Right Hand Rule states that the fingers will point in the direction of the magnetic flux. The magnetic flux intensity, H, at a distance S from the straight wire (considered as one turn) is[6]

$$H = I/(2\pi S) \tag{8}$$

where $2\pi S$ is the circumference. If this is substituted into (7), the result is,

$F = \mu L(I_1/2\pi S)I_2 = \mu HLI_2$; but $B = \mu H$, so that

$F = BLI_2$ or $F = 0.1BLI$ with I in amperes. (9)

Dynes = gausses x centimeters x abamperes.

---

[5]Ward, pp. 18-22

[6]Ward, p. 232.

It is not necessary, in order to use equation (9), that the field be produced by a parallel conductor or that the conductor upon which the force acts be long. It is only necessary that the conductor be perpendicular to the magnetic lines (or the perpendicular component used). The magnetic field may be produced by a permanent magnet or current-carrying conductors.

If a hand rule is used, this is applicable to motors although this is the force (plus other losses) overcome by the prime mover in turning a generator.

Since the mechanical engineer will likely want the force in pounds, equation (9) can be modified to use English units as follows:

Pounds x 0.4448×10^6 = dynes L cm x 2.54 = L inches

B lines/(cm^2 x 6.45) = B lines/in^2

$$F \text{ (lbs)} = \frac{\text{B lines} \times \text{L in.} \times 2.54 \times I \times 0.1}{in^2 \times 6.45 \times 0.4448 \times 10^6}$$

$$= 0.1 \text{ BLI}/(1.13 \times 10^6) = 0.885 \text{ BLI } 10^{-6} \text{ pounds} \qquad (10)$$

with B in lines per square inch, L in inches, and I in amperes. Again, only the perpendicular component of L with respect to the flux direction is effective.

C. FERROMAGNETISM, MAGNETIC CIRCUITS, AND PERMANENT MAGNETS.

A magnetic field exists in any space in which a current-carrying conductor is acted upon by a force. The earth itself is a gigantic magnet, but the fields most encountered by engineers are produced by a current in a coil of wire or by a permanent magnet.

Figure 3 shows how a toroidal winding produces the simplest magnetic field. If the turns are closely wound, it is found by experiment that very little of the field exists outside of the toroid. Although

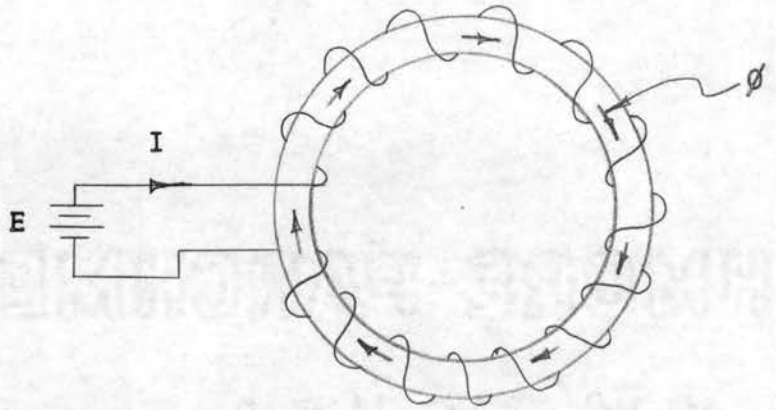

Figure 3. A toroidal coil produces the simplest magnetic field.

more flux density exists on the inner radius than on the outer radius, if the radius of the toroidal material is small compared with the overall radius, this may be neglected. The term, $0.4\pi NI$, is called the magnetomotive force (MMF). It drives a magnetic flux, ϕ, around the circuit containing a reluctance, $\mathcal{R}$. By analogy, the MMF, ϕ, and $\mathcal{R}$ are sometimes compared with emf, I, and R of an electric circuit. As with most analogies, this one is not particularly useful. For the simple circuit shown where the magnetic field and flux are parallel with the toroidal axis, and where leakage flux may be neglected, the magnetic flux density is defined as

$$B = \phi/A \tag{11}$$

where the flux density B, in lines (or maxwells) per square centimeter, is the total flux divided by the cross-sectional area. It is assumed here that the flux is normal to the area, and that the flux is of uniform distribution. The flux, ϕ, has been visualized as magnetic flux lines traveling around the magnetic circuit. In reality, nothing moves around the circuit as do electrons in an electric circuit. Flux lines, representing lines (or tubes) of magnetic force, are nothing more than an aid to visualization.

The magnetomotive force has been given as

$$MMF = 0.4\pi NI \text{ gilberts.} \tag{12}$$

The early physicists visualized 4π lines as emanating from a unit pole. The $4\pi NI$ has been divided by 10 to allow the use of the practical ampere instead of the abampere. For the toroidal coil shown in Figure 3, it will be found that the flux increases as the cross-sectional area increases and as L, the length of path, decreases. Hence,

$$\phi = \mu MMF\ A/L \tag{13}$$

where μ, called permeability, is a proportionality constant, or, as will be seen later, it is a property of the surrounding medium that measures the ease with which lines of flux are allowed to pass. If this equation is divided by A, then,

$$B = \phi/A = \mu\, 0.4\pi NI/L = \mu H \tag{14}$$

where H is the magnetic field intensity, related to B through μ. H has been used here as the magnetic potential gradient, that is, MMF per unit length, which is permissible for the simple toroidal circuit. In general, however, both B and H are vector quantities. It should be noted here that the permeability of a vacuum is unity, and very nearly unity for all nonmagnetic materials.

Equation (13) may be regrouped as

$$\phi = (\mu A/L)MMF = (P)MMF = MMF/\mathcal{R} \tag{15}$$

where P is the permeance and $\mathcal{R}$ is the reluctance of the magnetic circuit. These are similar to conductance and resistance in an electric circuit.

The analogy of magnetic circuit quantities with electric circuit quantities ends with its statement. There is no magnetic insulator so that magnetic flux may be kept in a specified space as electrons may be kept in a conductor (for all practical purposes) at reasonably low

frequencies. This is to say, leakage flux may not be neglected in the general case. Furthermore, the permeability, while a constant for air and nonmagnetic materials, is quite variable for the ferromagnetic materials. Magnetic circuits are, almost without exception, nonlinear, so that graphical methods rather than mathematical methods are commonly used.

If the toroid of Figure 3 is filled with a ferromagnetic material, it will be found that the flux will have increased several times over the case when air or a nonmagnetic material is used. This phenomena will be explained after some necessary terminology is given.

When a sample of ferromagnetic material is magnetized by the application of an external field, usually by current through a coil, the curve of B vs H rises nonlinearly as shown in Figure 4. Usually, the total induction, B, is plotted. However, some authors plot intrinsic induction, B_i, which is merely the total induction minus the induction had there been no iron present. It will be noted that the curve initially is concave upward, passes through a point of inflection, then becomes concave downward. As will be explained later, the "little magnets" in the iron furnishes the MMF for a major portion of the induction until such time as these have all been aligned with the applied field, after which the curve assumes a constant slope as if the sample were nonmagnetic thereafter. The greatest slope occurs at the point of inflection, and this is where maximum permeability, $\mu_m = B/H$, occurs. The maximum flux density, B_m, at point 2, is placed at the point of complete saturation, i.e., where the permeability equals one as in air. The curve from points 1 to 2 is called the virgin magnetization (or saturation) curve. If the magnetizing force now be decreased to zero, the curve falls to point 3, which is the

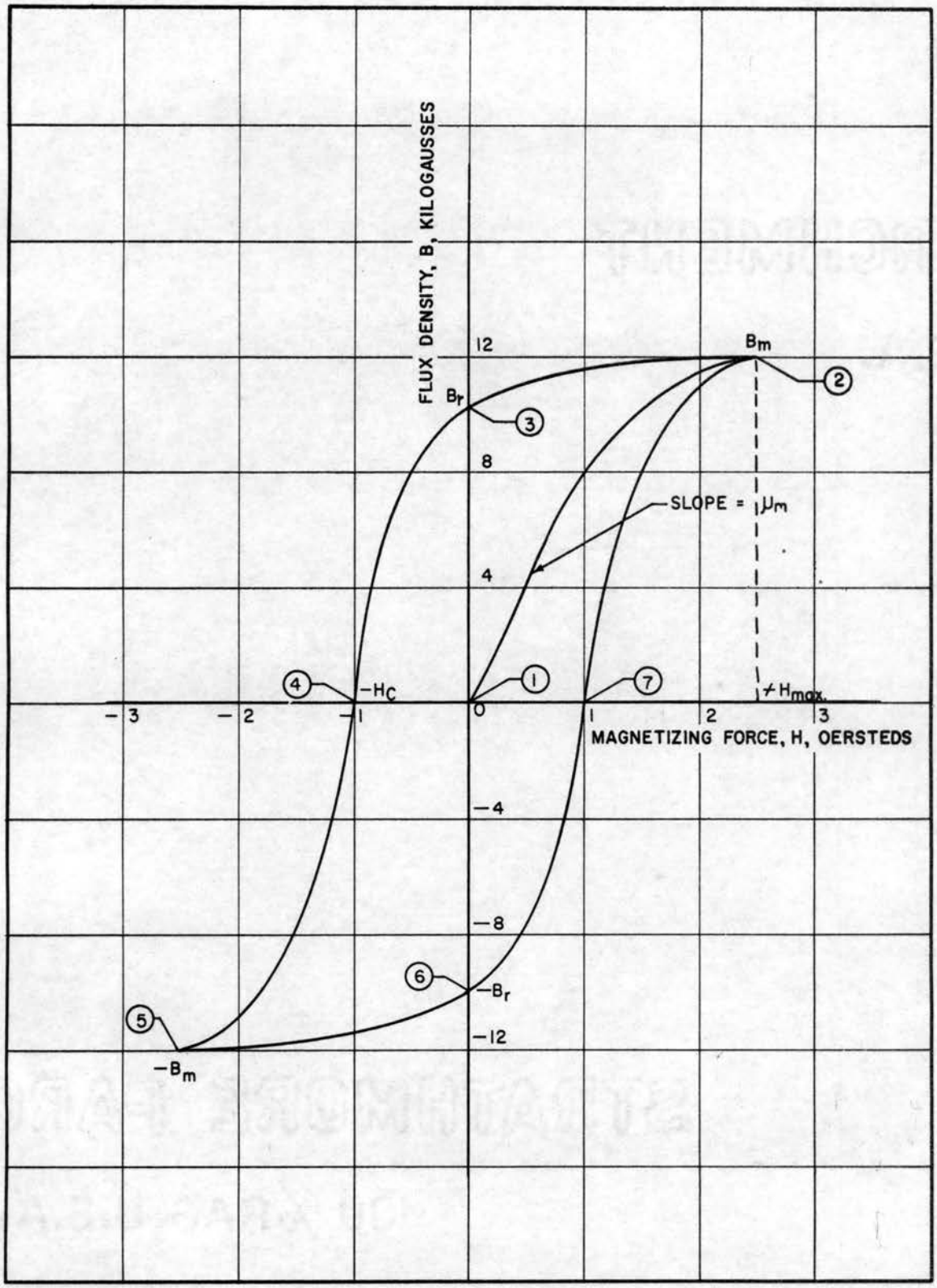

Figure 4. Virgin Magnetization Curve and Hysteresis Loop.

residual flux density, B_r. B_r is always B_r, but it is also called retentivity if B_m has been used. It is assumed here that the magnetic circuit is completely in iron, i.e., that there are no air gaps present. If the current is reversed in the magnetizing coil, and increased in the negative direction the curve falls to B = 0 at - H_c or point 4 on the figure. H_c is called the coercive force, being that magnetizing force required to reduce the residual flux density to zero. It should not be inferred that upon the removal of H_c the flux density remains at zero. It will return to some value along a minor hysteresis loop as will be explained later. As the current is increased in the negative direction to the same value as used in the positive direction the curve will reach point 5 at a negative B_m. As the current is reduced to zero, B goes to - B_r at point 6. When the current is again increased in the positive direction the curve will pass through point 7, and on to point 2, to complete what is called the hysteresis loop. The loop is symmetrical and the material is said to be in a cyclic condition when the maximum current is reversed several times. If this is not done the loop will not close. An example of the saturation curve and hysteresis loop will be found further along in this report for the iron used in the pole piece contained in the generator frame. The phenomenon of the flux density lagging the applied magnetizing force is known as hysteresis, there being two values of B for most values of H. The lag is not a time lag. The area of the hysteresis loop is proportional to the so-called hysteresis loss in the sample (may be likened to molecular friction) manifested as heat.

Contrasted with permeability, normal permeability is defined as B/H when the sample is in a symmetrically cyclically magnetized condition, i.e., the induction in the positive direction is equal to the induction in

the negative direction so that the hysteresis loop closes.[7] However, some designers use the permeability obtained from the saturation curve.

A partial explanation of ferromagnetism will now be given. For a complete treatment of this subject the reader should refer to the book by Bozorth, containing 968 pages of which 72 pages are bibliography alone with 1729 references cited for the period 1842 to 1951. The material presented here is from the book by Bozorth,[8] an article by Bozorth,[9] and from a book by Ward.[10]

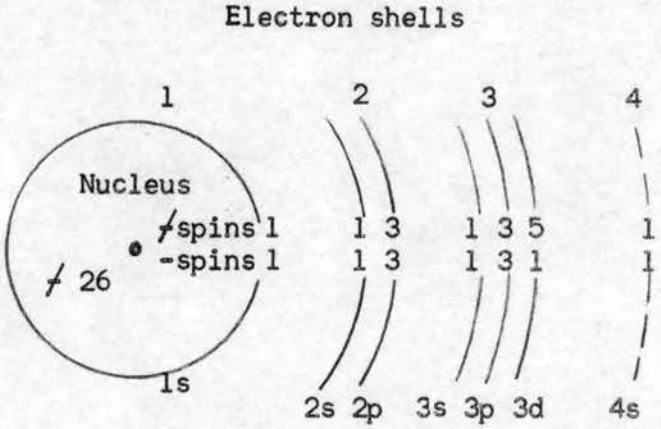

Figure 5. Electron shells in a free-iron atom.

The arrangement of the 26 electrons in a free-iron atom in more or less well-defined shells is shown in Figure 5. The magnetic moment of the atom (defined as $M_0 = ef\pi r^2/c$, where e is the charge, f is the num-

---

[7] Standard Definitions of Terms, with Symbols, Relating to Magnetic Testing, American Society for Testing Materials, ASTM Designation A340-49, (Philadelphia, 1949).

[8] Richard M. Bozorth, Ferromagnetism, (New York, 1951), pp. 476-479.

[9] Richard M. Bozorth, "The Physics of Magnetic Materials," Electrical Engineering, Vol. 75, February, 1956, pp. 134-140.

[10] Ward, pp. 183-184.

ber of spins around the nucleus per second, r is the radius of the orbit, and c is the velocity of light) is not of prime importance in ferromagnetism. The magnetic moment of importance (in ferromagnetism) is that of the SPINNING electron which is known to have a moment of 0.927×10^{-20} in CGS units or 1 Bohr magneton (from quantum theory). This is contrary to the impression left by some text books because it is so easy for the student to reason that Ampere's Right Hand Rule for finding the flux direction may be applied by using the electron's path as current direction. The conventional current direction, of course, is opposite to electron flow.

The spins of the two electrons in shell 1 are such that the magnetic moments cancel, leaving a net moment of zero. However, it will be noted that the third shell is not completely filled so that complete neutralization is not realized. The atomic moment of atoms and ions of iron, cobalt, and nickel can be attributed to the unbalanced spins of their 3d electrons. In the free atom of iron the moment should be the difference between the five 3d $\nearrow$ spins and one 3d - spin or 4 Bohr magnetons. In metallic iron with many atoms, the net atomic moment is reduced to 2.2 Bohr magnetons due to the changed distribution of electrons because of the close proximity of neighboring atoms.

The theory that a ferromagnetic material is composed of many regions, called domains, each magnetized to saturation in some direction, was first stated by Weiss in 1907, and is accepted today with some modifications. The atoms appear to be grouped magnetically into domains (may contain as many as 10^{15} atoms) and so aligned that their magnetic effects are all in the same direction. The atoms are interlocked within the domain so that the realignment of any must mean the realignment of all. In this

way a single, large magnetic moment is substituted for a larger number of small independent moments. In the unmagnetized state, the directions in which the domains are saturated are distributed at random in such a way that the resultant magnetization of the sample is zero. Application of an external field changes only the direction of magnetization, not the magnitude. Figure 6 shows the body-centered space-lattice of iron. The

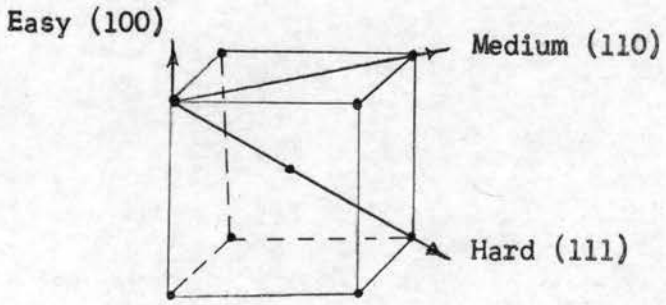

Figure 6. Magnetic properties and structure of a single iron crystal.

normal direction of alignment of any particular domain is parallel to the edges of the cubes which make up the space lattice in what is called by crystallographers as the 100 direction. The face diagonal is the 110 direction, and the cube diagonal is the 111 direction. When a small external magnetic field is applied to an iron sample, one-half of the domains in the 100 direction are already aligned with the external field. As the external field is increased the remainder of the 100-direction domains readily realign. These domains in the 110 and 111 directions are more difficult to align, but as the field is increased they change first to the 100 direction nearest to the direction of the field, and gradually allow themselves to be oriented closer and closer to the field direction. When all of the domains have been aligned the condition of saturation exists. The B-H curve from this point on is a straight line, as if the volume of iron were nonmagnetic.

The above remarks do not purport to go very far into the theory of

ferromagnetism, but are intended only as an introduction to the subject. It should also be noted that some of the statements apply only to iron.

If a sample of iron be subjected to cyclic magnetization, a voltage is induced, and currents will flow since ferromagnetic materials are electrical conductors. These currents give rise to eddy-current losses in addition to the hysteresis losses previously mentioned. While hysteresis loss, $P_h = K_h f B_m^x V$, (where K_h is a constant for a material, f is the frequency, B_m is the maximum induction, x is the Steinmetz exponent, and V is the volume of the sample) is proportional to the frequency, the maximum flux density to some power, and to the volume, the eddy-current loss is given by $P_e = K_e f^2 c^2 B_m^2 V$ ONLY for thin, laminated samples where c is the lamination thickness. This formula will not be applicable to the generator in this work, but it is useful in that it shows that eddy-current loss goes up rapidly with frequency and the maximum flux density.

Magnetic circuits are solved in a manner similar to electric circuits except that there are leakage fluxes with which to contend. Without exception, the literature and texts are in accord with one item, and that is that the solution or design of magnetic circuits dealing with leakage flux comes only with long experience. Since this work is mostly concerned with permanent magnets, electromagnetics will not be considered in detail.

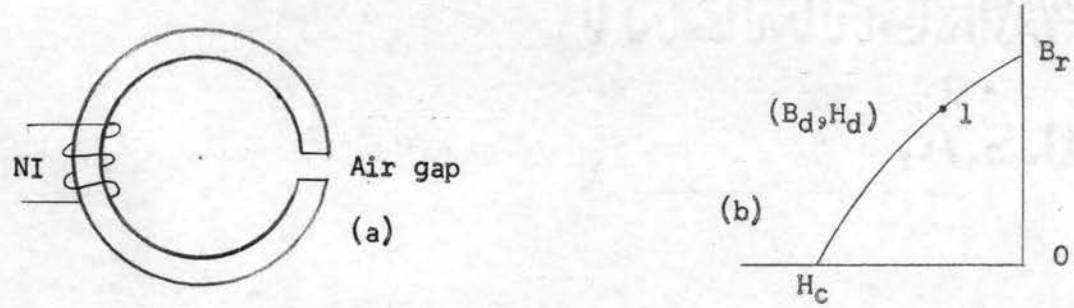

Figure 7

Suppose that, in Figure 7 (a), a MMF in the form of a current is

applied to the coil around a permanent-magnet material while the air gap is closed with a piece of soft iron. When the current is removed the flux density will fall to some B_r shown in Figure 7(b). When the soft iron is removed to place the air gap in the circuit, the flux density will drop to some point 1 marked (B_d, H_d). Only that part of the hysteresis loop in the second quadrant, known as the demagnetization curve, is shown in Figure 7(b). The flux now in the circuit is supplied by the domains remaining in alignment in the iron. The iron becomes the source of MMF equal to the drop in magnetic potential across the air gap provided leakage flux is neglected. Using a sort of a Kirchhoff's Law for magnetic circuits, i.e., a summation of magnetic potential rises and drops around a circuit, $H_mL_m = H_gL_g$, considering H_mL_m as a rise and H_gL_g as a drop in the magnet and in the air gap, respectively. In air, $H_g = B_g$ when the CGS system of units is employed. Since leakage flux is being neglected, the flux in the iron must be equal to the flux in the gap. In these equations, L is a length and A is a cross-sectional area normal to the flux direction. These equations are numbered for reference:

$$H_mL_m = H_gL_g = B_gL_g \tag{16}$$

$$B_mA_m = B_gA_g \tag{17}$$

With the use of demagnetization curves, these equations may be solved by a trial-and-error method.

Since leakage flux should not be neglected, formulas will be developed as given by Spreadbury.[11] For the electromagnetic counterpart, the reader may consult Roters.[12] Figure 8 shows the construction details

---

[11]F. G. Spreadbury, Permanent Magnets, (London, 1949), Chapter IV.

[12]Herbert C. Roters, Electromagnetic Devices, (New York, 1941).

of a generator frame used as an experimental model to check the theory and to obtain an idea as to the weight of the coil frame and coil for the prime mover force requirement calculations. Theoretical and experimental results will be considered in Chapter IV.

The reluctance of a magnetic circuit is defined as MMF/ϕ. Substituting HL = MMF, ϕ = BA, and H = B/μ,

$$\mathcal{R} = HL/BA = BL/\mu BA = L/\mu A \qquad (18)$$

which shows that reluctance is fundamentally a length over an area. This is further simplified in air and other nonmagnetic materials simply as length divided by area since μ equals unity.

Magnetically, air is a poor insulator, and whenever a magnetic potential difference is formed therein, a leakage flux will occur.

Dimensions in centimeters.
N is the neutral point of the permanent magnet.

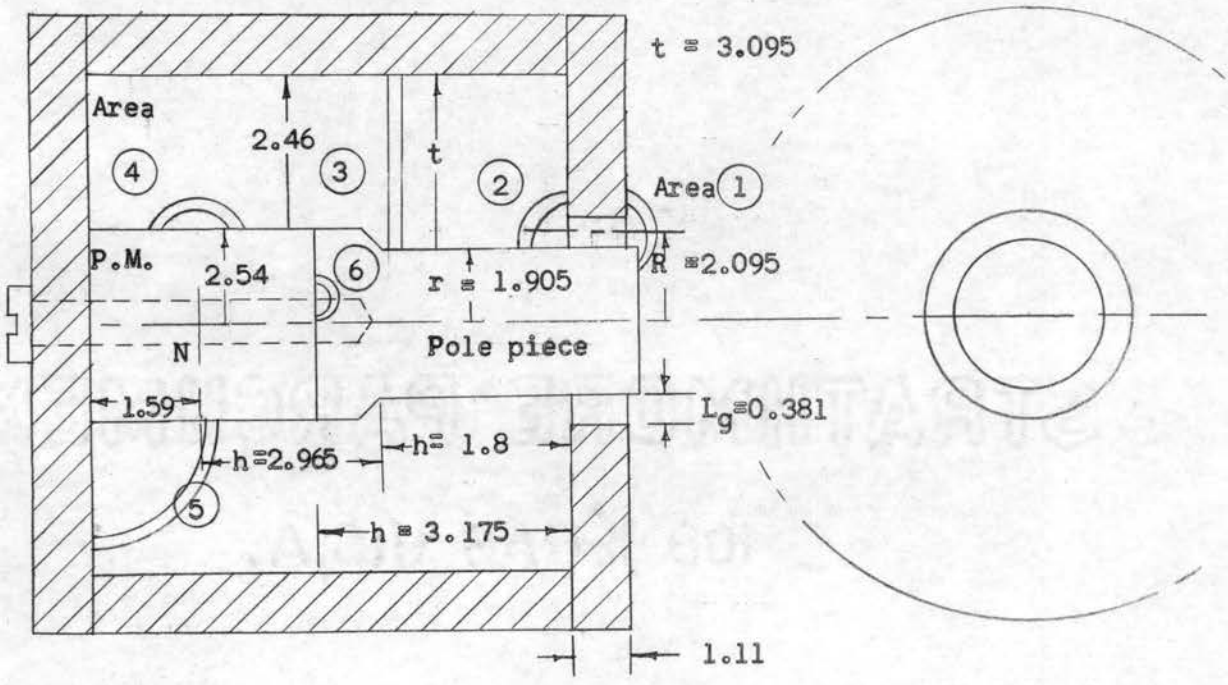

Figure 8. Experimental generator frame details, showing leakage flux paths. (Not drawn to scale)

Due to the properties of variable reluctance and leakage, the determination of the flux in a magnetic circuit is a far less simple matter than the determination of the current in an electric circuit. There is leakage flux from every point of the magnetic circuit except at N, the neutral point of the magnet. If the leakage flux were confined to a simple, definite path, the determination of the reluctance of this path would be easy. It is seen that a magnet has not only to provide the useful flux in the air gap, but also that flux not passing through the air gap, usually all lumped together as leakage flux. Usually, the leakage flux is greater than the useful flux so that the practice of neglecting leakage flux, as in elementary texts, cannot be used. It is evident from equation (18), that to decrease the leakage flux by increasing the reluctance, the leakage path should be large and the area small. Also, magnets with large areas tend to produce large leakage fluxes. The Alnico group of permanent magnet material is useful in that for a given performance the volume of material required is considerably less than when a steel is used. The leakage flux from the magnet surface is termed surface leakage, and the leakage flux from the ends is known as terminal leakage.

If an error is made in predicting the leakage flux in electromagnets, the winding can be changed; whereas, in permanent-magnet circuits, an error calls for a structural change.

The difficulty of estimating leakage is due to the fact that it is impossible to say exactly what paths the leakage flux will follow. A knowledge of the paths would involve a knowledge of the configuration of the lines of force bounding these paths. This problem has not been solved. Such leakage formulas as exist are based on the assumption that actual lines of force may be replaced by curves of simple geometrical figures.

Some formulas applicable to the shape of the generator frame shown in Figure 8 will now be given, some derived and others stated. Unless otherwise stated these are due to Spreadbury as noted in footnote 11.

With reference to Figure 9, the leakage flux for area one may be

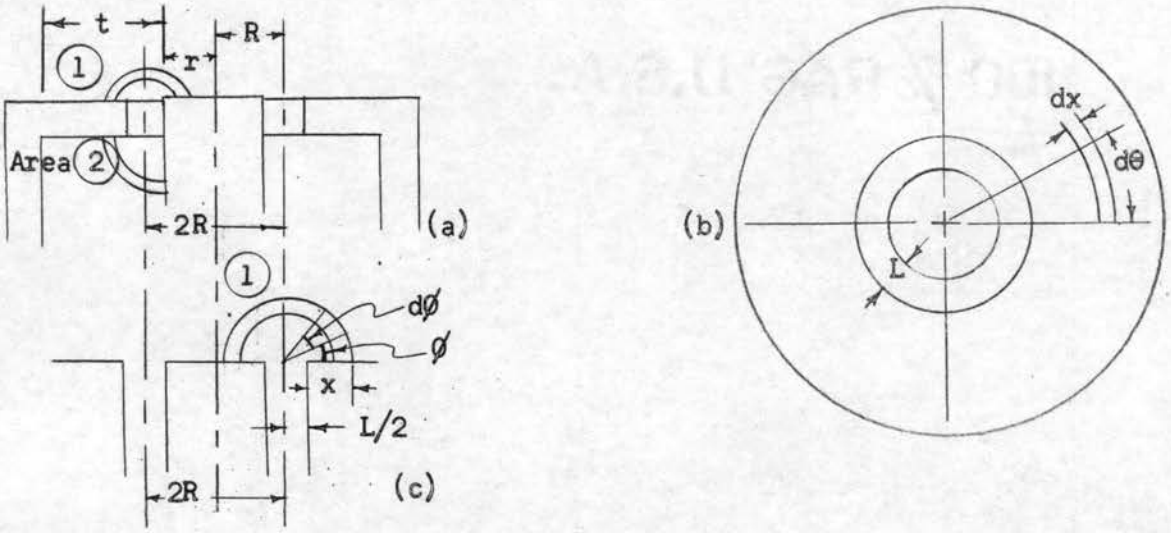

Figure 9

regarded as following semi-circular paths. The length of the path is $\frac{1}{2}\pi D = \pi$ radius $= \pi(x \neq L/2)$. An elementary area is circumference times width $= Rd\theta dx$, where $Rd\theta$ is arc length along circumference.

Permeance, $p = 1/\mathcal{R} = A/L$; $\qquad dp = \dfrac{Rd\theta dx}{\pi(x \neq L/2)}$.

$$p = \frac{1}{\pi}\int_{L/2}^{R}\int_{0}^{2\pi}\frac{Rd\theta dx}{x \neq L/2} = \frac{R}{\pi}\int_{L/2}^{R}\frac{dx}{x \neq L/2}\int_{0}^{2\pi}d\theta$$

$$= R/\pi\left[\ln(x \neq L/2)\right]_{L/2}^{R}\left[\theta\right]_{0}^{2\pi} = R/\pi\left[\ln(R \neq L/2) - \ln(L/2 \neq L/2)\right](2\pi)$$

$$= 2R\left[\ln(r \neq L/2) - \ln L\right] = 2R\left[\ln\frac{(r \neq L/2)}{L}\right] = 2R\ln(R/L \neq \tfrac{1}{2}).$$

$$\mathcal{R} = 1/p = \frac{1}{2R\ln(R/L \neq \frac{1}{2})} \qquad \text{Note: Use logarithm to base e.} \qquad (19)$$

Apparently, author Spreadbury is in error with $\mathcal{R} = \dfrac{1}{2R\ln(2R/L \neq 1)}$.

The formula ignores the area beyond a radius 2R where the flux is rela-

tively weak.

The leakage paths on the under side of the plate consist of quadrants. This reluctance is

$$\mathcal{R}_2 = \frac{\pi}{4[\pi r \ln t/L + 2(t - L)]} \tag{20}$$

Figure 8 shows area three leakage path, which is radial between the center pole piece and the annular yoke.

$dL = dx$; $dA = 2\pi \text{radius } h = 2\pi h(x + r + L)$.

Then, $d\mathcal{R} = \frac{dx}{2\pi h(x + r + L)}$; $\mathcal{R} = 1/(2\pi h)\int_{-L}^{t-L} \frac{dx}{(x + r + L)}$

$= 1/(2\pi h)\left[\ln(x + r + L)\right]_{-L}^{t-L} = 1/(2\pi h)\left[\ln(t - L + r + L) - \ln(-L + r + L)\right]$

$$\mathcal{R}_3 = \frac{\ln\left(\frac{t + r}{r}\right)}{2\pi h} \tag{21}$$

Later on, a comparison will be made of the flux calculated with these formulas and that flux measured experimentally. Where necessary, a correction factor will be applied to the formulas.

Figure 10 shows the demagnetization and external energy curves representing an Alnico 5 permanent-magnet material. After the initial magnetizing force is removed from the magnet assembly, the flux falls to B_r. When the soft iron keeper is removed from the air gap the flux drops to some point A. If the assembly is now subjected to a demagnetizing force, B_d moves along the curve from A to B. Upon removal of this force, the point moves to point C. If this procedure is repeated, a minor hysteresis loop is traced as shown by the dashed lines between A and C. As can be seen, this hysteresis loss is very small. Many designers use the straight line joining the points. Instead of the initial demagnetizing force, suppose that the magnet were open-circuited so that B_d moved from A to D. If the magnet is now replaced in the assembly with the air gap,

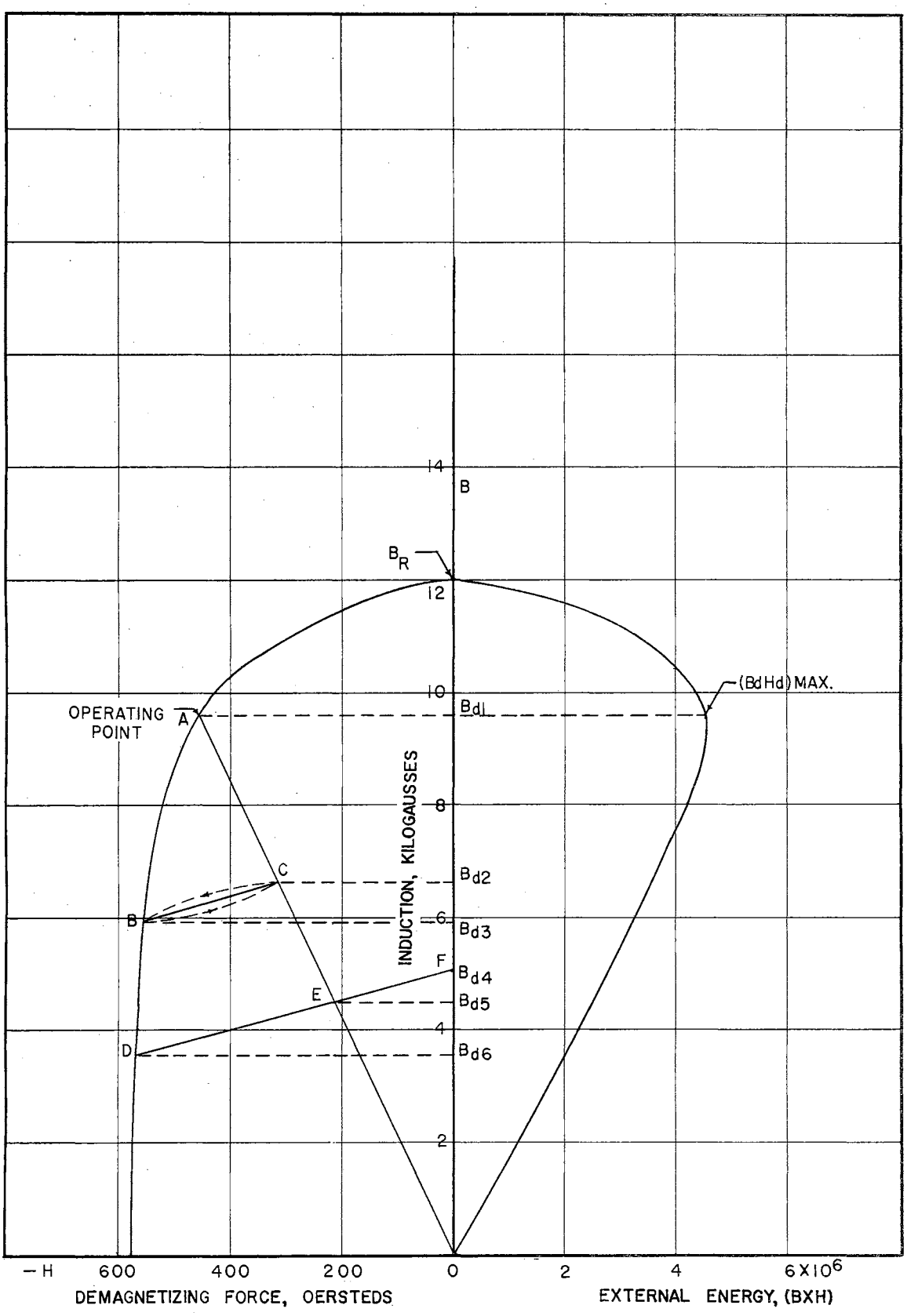

Figure 10. Demagnetization and External Energy Curves for Alnico 5.

the operating point moves to point E. Had the air gap been eliminated also, the operating point would have moved to point F. It can now be seen that if a negative coercive force equal to $-H_c$ had been applied to reduce B_d to zero, removal of H_c would not have left the magnet demagnetized. In any event, a loss of flux density occurs when a demagnetizing force operates upon a magnet. It can now also be seen that magnets should be magnetized in the assembly, and not magnetized and placed in the assembly.

In the CGS system, the energy per cubic centimeter in the air gap and in the magnet material is $BH/8\pi$ ergs. In addition to B_r and $-H_c$, manufacturers of magnets use $B_dH_{d\ max.}$ as a measure of merit of a material. An external energy curve from the product, B_dH_d, (omitting the 8π), is shown in Figure 10. For the most efficient magnet (i.e., for the least volume of magnetic material), the assembly should be designed to operate at point A where B_dH_d is a maximum. Using equations (16), $H_mL_m = H_gL_g = B_gL_g$, and (17), $B_mA_m = B_gA_g$, and neglecting leakage for the moment:

From (17), $A_m = B_gA_g/B_m$;

From (18), $L_m = B_gL_g/H_m$; multiply both sides by A_m, for

$$A_mL_m = V_m = \frac{B_gL_gB_gA_g}{H_m\ B_m} = \frac{B_g^2\ L_gA_g}{B_mH_m} \qquad (22)$$

The volume of the magnet is the least when B_mH_m is the largest.

Point A shows a static operating condition. Since magnets are subject to various demagnetizing influences (shock, temperature variation, external magnetic fields, structural or metallurgical aging), it is desirable to deliberately demagnetize the magnet a certain amount that will surely be in excess of any that may be encountered. This is called stabilization. For example, if the assembly is demagnetized to point B, and recoils to

point C, the assembly will operate along BC as long as it is not subjected to demagnetization greater than that applied to move to point B. The line, OA, is called the shearing line (sometimes the load line or air gap line), and the line BC is called the recoil line. A magnet operating along DF is said to be in full-recoil. Recoil lines are all very nearly parallel to the tangent to the demagnetization curve at B_r. The slope of the recoil line is known as the reversible permeability.

Variable reluctance machines, such as rotating generators, pose complicated design problems that need not be considered here. However, the oscillating generator will have some demagnetizing influence so that the assembly will have to be stabilized. Needless to say, perhaps, but this process removes the design from the static case so that the magnet will not operate at the $B_dH_{d\ max}$. point.

Due to surface leakage, a magnet does not operate at the same B_d and H_d throughout its length, but this is neglected by magneticians. Equations (16) and (17) will now be re-written to take into account the fact that leakage flux exists.

$$H_mL_m = fH_gL_g = fB_gL_g \text{ in air gap;} \tag{23}$$

$$B_mA_m = FB_gA_g = FH_gL_g \text{ in air gap.} \tag{24}$$

F is a leakage factor, total flux/gap flux, so that when F times the air gap flux is used, there results the total flux. According to Bozorth,[13] small f is a leakage factor that takes into account the fact that the flux in the gap is not everywhere perpendicular to the pole face, and therefore the length of the path is somewhat greater than the geometrical value, L_g. In practice, f is between 1 and 1.5. A pamphlet issued by

---

[13]Bozorth, p. 362.

the General Magnetic Corporation[14] states that f is the reluctance of the circuit other than that in the air gap. Thomas & Skinner[15] makes an equivalent statement, but Carboloy[16] uses f = (Magnet MMF)/(MMF in the useful air gap). Spreadbury[17] states that f is expressed as a fraction of the magnetic potential drop across the gap, i.e., if f = 1.1, the drop through the iron portions of the circuit is 10% of the drop across the air gap. Except for Bozorth's explanation, these are all ways of saying the same thing. In any event, f and F are empirical factors used with equations (23) and (24) to obtain useful results. They are obtained experimentally or estimated after considerable experience as a magnetician.

---

[14] Alnico Permanent Magnets, General Magnetic Corporation, (Detroit, no date given), p. 4.

[15] Permanent Magnets, Thomas & Skinner Steel Products Company, Inc., (Indianapolis, 1955), p. 8.

[16] Alnico Permanent Magnet Design Manual, Carboloy Department of General Electric Company, (Detroit, 1955), p. 14.

[17] Spreadbury, p. 155.

CHAPTER IV

PRELIMINARY MODEL

It was early recognized that a model was necessary to gain knowledge since all of the literature emphasized that magnet design was largely empirical rather than anything like a science. Also, in this case, the designer of the prime mover needed an approximate weight of the coil and coil frame for design purposes. A coil cannot be oscillated in the field in an air gap similar to that shown in Figure 7(a), since induced voltages would cancel. From equation (5), $e = NBLv10^{-8}$ volts, which can be written as $e = BLv10^{-8}$ volts when the total length of the coil is used for L instead of an average length L times N turns, it can be seen that a high value of B, and a long coil of wire, along with a high velocity, would produce a high voltage. B will be limited by the material available, L will be limited by the coil space available, and velocity, v, will be influenced by a physical limitation, namely, inertia of weight. Figure 8 shows an acceptable layout because B, L, and v are mutually perpendicular, eliminating multiplication by sines or cosines to obtain perpendicular components of B, L, and v.

The yoke and permanent magnet materials were obtained from the machine shop scrap pile, and were totally unknown as to composition. Later, however, it was found that the permanent magnet material could only be Alnico 5. Figure 10 shows that hysteresis loss will be negligible. Eddy current loss may not be negligible, but it was not immediately seen

how this loss might be separated from the total losses. Lamination of core material is of great help in reducing eddy current loss, but introduces fabrication problems with available equipment.

Since the coil weight has to be small in order to be oscillated at a high rate (a formidable disadvantage compared with rotating equipment) the air gap can be small, a decided advantage in magnetic circuits. Large air gaps prevent obtaining a large value of flux density.

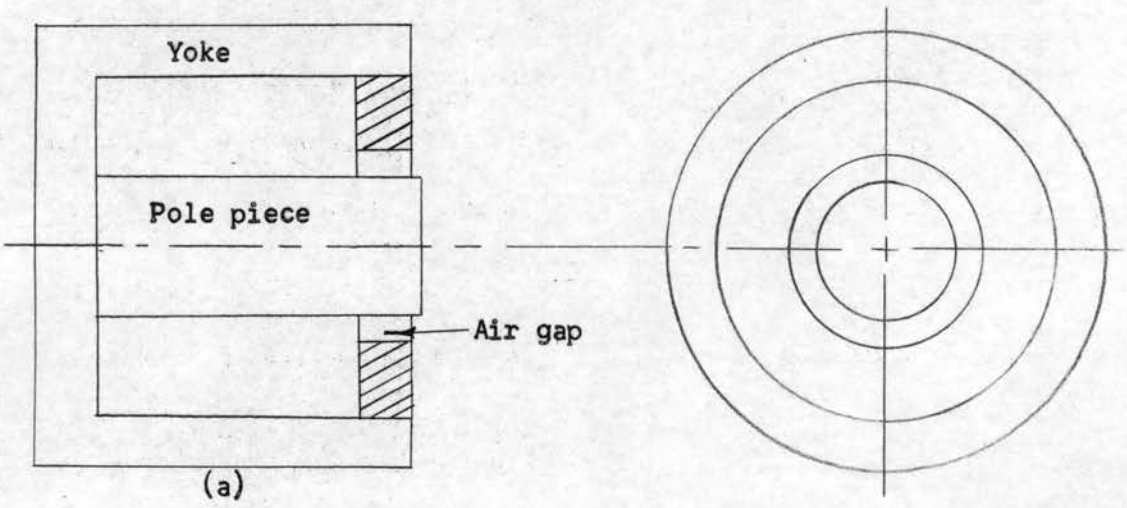

Cross-hatched areas represent permanent magnet materials.

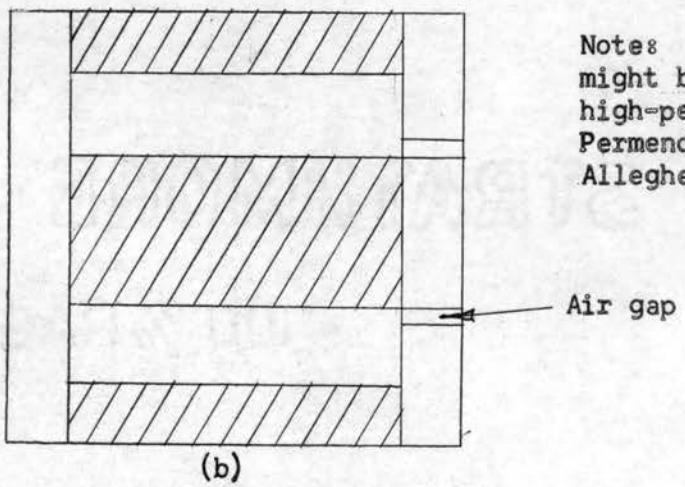

Note: Part of the iron portions might be constructed of laminated, high-permeability material such as Permendur as manufactured by the Allegheny Ludlum Steel Corporation.

Figure 11. Permanent magnet and yoke assembly designs.

Figure 11(a) shows an assembly design that will produce the least leakage flux. However, the high energy product materials Alnico 5, 6, and 7 may not be used since these materials are anisotropic, that is, after heat treatment in a magnetic field, they must be magnetized in the same direction as when under heat treatment; otherwise, the high B_r associated with these materials is reduced by a factor of 4 to 7. The nondirectional Alnico 12, with a B_r of 5.5 kilogausses, might be used, and possibly yield a higher flux density in the air gap than Alnico 5 with a B_r of something over 12 kilogausses. Since Alnico 12 is so brittle, Alnico 2 might be the better choice of material. Figure 11(b) shows a promising design utilizing two ring magnets. Here, Alnico 5 could be used.

The physical layout shown in Figure 8 was most easily constructed with the materials available at the time. With this assembly, 230 turns of number 14, heavy formex wire were wound around the magnet and partly around the raised shoulder of the pole piece for magnetizing purposes. A hand gaussmeter measured 1.2 kilogausses in the air gap before magnetizing the magnet in the assembly. Prior to magnetizing, a soft iron keeper was placed so as to eliminate the air gap. Manufacturer's data show that 3000 oersteds (times 2.02 = ampere turns per inch in English units) per centimeter of length of magnet are required to saturate the material at about 16.3 kilogausses. This is 6060 NI/inch, and this times 1.25-inch length of magnet used, yields 7575 NI/inch. To provide for external reluctance and unknown factors a current of 65 amperes (d.c.) at 33 volts was used to magnetize. This was 65 x 230 = 14,950 NI/inch, a value high enough to insure saturation. After removal of the shorting iron (quite difficult due to forces involved) the following flux measurements in the air gap with the gaussmeter were made: 4.48, 4.55, 4.35, and 4.3 kilogausses

at 12, 3, 6, and 9 o'clock, respectively. These were later found, by the use of a pull-off coil, to be maximum values instead of average values. Rectangular coils and pull-off coils of various dimensions and number of turns were tried. The only usable coil was found by experiment to be a one-turn pull-off coil that just slipped over the pole piece. These coils were used with a light-beam type fluxmeter to measure flux. (For information on this type of fluxmeter, see the General Electric Company pamphlet on the instrument.) The following figure shows the results of this test.

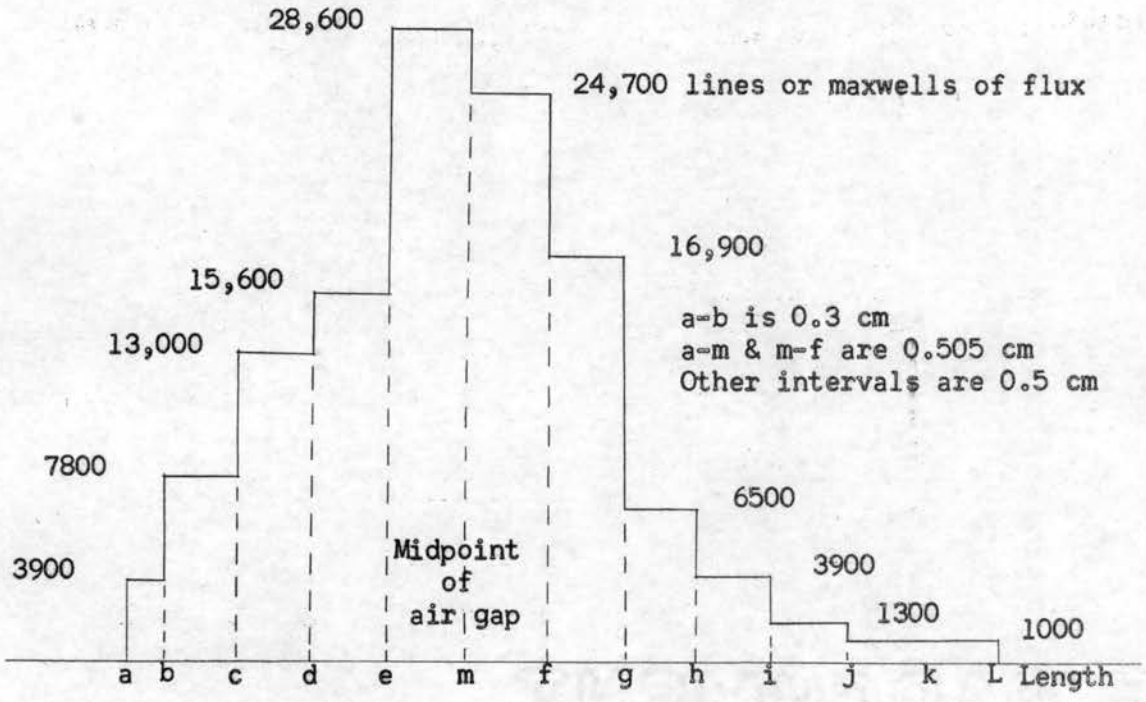

Figure 12. Results of flux measurements along pole piece, using one-turn pull-off coil of #30 wire. (Not to scale)

Total pull-off gave 120,800 lines. In the step pull-off indicated in Figure 12, the results were, a to b plus b to c plus c to d plus d to e, 40,300 lines; e to m plus m to f (the 1.11 centimeter-deep air gap), 53,300 lines; f plus the increments to L, 31,200 lines. The summation of all increments yielded 124,800 lines as compared to 120,800 lines

found with total pull-off. Since the area of the air gap was 13.28 square centimeters, the flux in the gap was (28,600 / 24,700)/13.28 = 53,300/13.28 = 4010 gausses or 4.01 kilogausses. It was seen that the gaussmeter previously mentioned was reading the value of B between e and m, namely, (28,600 x 2)/13.28 = 4310 gausses.

Since it appeared that B_g was greater on the inside of the assembly than on the outside, it might be desirable to place a slight taper on the air gap surface of the front plate.

Figure 12 vividly portrays the fact that leakage flux cannot be neglected, and that the leakage flux is considerably more than the flux in the air gap.

A nominal difference of 50 gausses, by the gaussmeter, was noted between the pole piece and front plate gap surface area. In other words, along the radial gap length, L_g, B_g was essentially constant.

Using the physical dimensions shown in Figure 8, and the reluctance formulas previously given (plus other data as indicated), calculated and experimental values of flux were compared to determine the utility of the reluctance formulas.

From equation (19): $\mathcal{R}_1 = \frac{1}{2R\ln(R/L + \frac{1}{2})} = \frac{1}{2x2.095\ln(2.095/0.381 + \frac{1}{2})}$

$= 1/\left[4.19\ln(5.5 + 0.5)\right] = 1/(4.19 \ln 6) = 1/(4.19 \times 1.79) = 1/7.5 = 0.1333$ reluctance units. Using equation (16), $H_gL_g = B_gL_g = 4310 \times 0.381 = 1642$ gilberts. The inside flux density was used as all other paths were in parallel. $\phi_1 = MMF/\mathcal{R} = 1642/0.1333 = 12,600$ lines as compared with 31,200 lines found with the pull-off coil. This reluctance formula cannot be used. The ratio, $\phi_1/\phi_g = 31,200/53,300 = 0.585$, will be used with new designs.

From equation (20): $\mathcal{R}_2 = \frac{\pi}{4[\pi r \ln t/L + 2(t - L)]}$

(Note: To coincide with the range of pull-off coil, which was inserted only 1.8 cm from inner surface of front plate due to interference of the pole piece shoulder, t = 1.8 was used.)

$$\mathcal{R}_2 = \frac{0.7854}{5.98 \ln 4.725 + 2.858} = 0.0647.$$

Partial ϕ_2 = MMF/$\mathcal{R}$, = 1642/0.0647 = 25,400 lines. The value found for area two leakage flux, when corrected as shown below, was 43,300 lines.

From equation (21): $\mathcal{R}_3 = \frac{\ln(t + r)/r}{2\pi h} \quad \frac{\ln(3.095 + 1.905)/1.905}{2\pi 1.8}$

= 0.0854 reluctance units, using h = 1.8 cm for comparison with experimental results. Partial ϕ_3 = (1642/2)/0.0854 = 9630 lines.

The sum of ϕ_2 and ϕ_3 = 25,400 + 9630 = 35,030 lines. By pull-off coil, the lines were found to be 40,300. The error was 40,300 - 35,030 = 5270 lines. The percent error was 5270 x 100/40,300 = 13.05%. Assuming that the error was all in area two formula, the usual result will be divided by 0.87 for the corrected area two leakage flux.

The following derivation of radial leakage flux in the space occupied by the coil is due to Still.[18] Refer to Figure 13. The leakage flux depends not only upon the permeance of the air path, but also upon the MMF tending to establish a magnetic flux. This MMF is no longer a constant value, but, on the assumption that the reluctance of the iron paths is negligible, it will increase according to a straight-line law from zero when x = 0 to a maximum when x = h.

---

[18]Alfred Still, Elements of Electrical Design, (New York, 1924), p. 77.

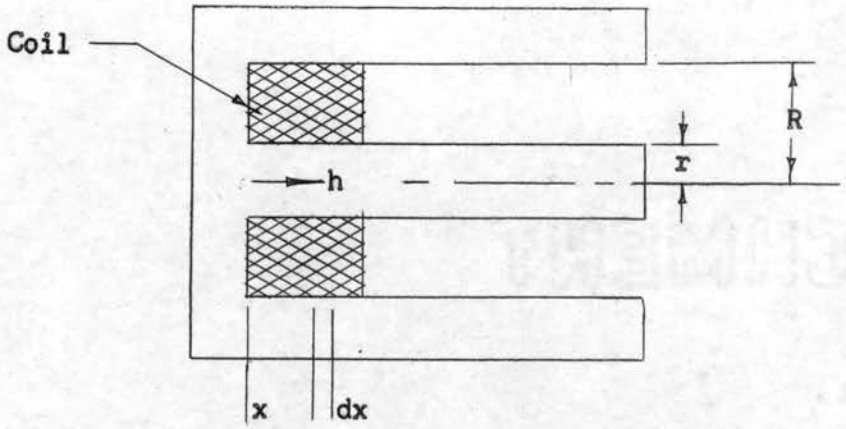

Figure 13. Radial flux leakage.

ϕ = MMF x P, where P is the permeance.

$d\phi = (0.4\pi NI\ x/h)\ (2\pi dx/\ln R/r)$.

$$\phi = 0.4\pi NI \times 1/h \times \frac{2\pi}{\text{Ln}R/r} \int_0^h x\,dx = \frac{0.4\pi NI}{h} \frac{2\pi}{\text{Ln}R/r} (h^2/2)$$

$$= \frac{0.4\pi NI}{2} \times \frac{2\pi h}{\text{Ln}R/r} . \qquad \mathcal{R} = 1/P = \frac{\text{Ln}R/r}{2\pi h}$$

This formula is the same as that given by Spreadbury[19] where R = t + r. The result is ϕ = average MMF x permeance, or average MMF divided by reluctance.

This cannot be applied directly to a permanent magnet, but it seems reasonable to extend h in Figure 13 to the magnet midpoint or magnet neutral, N. MMF will be that of the air gap divided by two because the reluctance drop in the iron has been assumed negligible.

The pole piece and magnet were 5.08 cm in diameter in the region under consideration (remainder of radial leakage, area three, beyond that found out to h = 1.8 cm).

---

[19]Spreadbury, p. 101.

$$\mathcal{R}_3 = \frac{\ln(t \neq r)}{2\pi h} = \frac{\ln 5/2.54}{2\pi 2.965} = 0.0362 \text{ reluctance units.}$$

$\phi_{3(part)} = (1642/2)/0.0363 = 821/0.0363 = 22{,}650$ lines.

Area four is for surface leakage. Adapting the information in Figure 4-2 in Spreadbury,[20] (flux density in magnet and loss in flux density is plotted versus magnet length from neutral) the leakage ratio is 200/2700 = 0.074 or about 7%. The summation of flux for all other areas will be divided by 0.93 to obtain an approximation of the total flux.

Area five leakage flux was computed using area two formula, but t = 2.46 cm, and L = 1.59 cm. The reluctance was found to be 0.1505 reluctance units. Hence, $\phi_5 = 1642/0.1505 = 10{,}900$ lines. Applying the correction factor, the result was $10{,}900/0.87 = 12{,}530$ lines.

Area six is the 3/8-inch hole through the magnet, and is occupied mainly by the brass holding bolt. The area was 0.713 $cm,^2$ and the length was 3.18 cm. $\mathcal{R}_6 = L/A = 3.18/0.713 = 4.46$ units. This was quite large compared with the other reluctances, so that this leakage flux was neglected.

The summation of the fluxes, $\phi_g = 53{,}300$, $\phi_1 = 31{,}200$, $\phi_2 = 43{,}300$, $\phi_{3\ part} = 9630$, $\phi_{3\ part} = 22{,}650$, $\phi_5 = 12{,}530$, was 172,610 lines. Allowing for surface leakage, the total flux, $\phi_t = 172{,}610/0.93 = 185{,}500$ lines through magnet neutral. $B_m = 185{,}500/19.54 = 9.49$ kilogausses.

$H_m = 568$ oersteds from an Alnico 5 demagnetization curve. $H_m L_m = 568 \times 3.18 = 1810$ gilberts, as compared to 1642 for the air gap. H_m is in a region on the curve where H_m is changing rapidly so that a small

---

[20] Spreadbury, p. 90.

error will be magnified.

The leakage factor, F, was $F = \phi_t/\phi_g = 185{,}500/53{,}300 = 3.48$. The reluctance factor was $f = H_m L_m / H_g L_g = 1810/1642 = 1.1$. These values seemed reasonable so that model number one could be designed.

CHAPTER V

OPTIMUM PERMANENT-MAGNET ASSEMBLY DESIGN

A large number of permanent magnet materials are available, some having a larger residual flux density than the Alnicos, some having a larger coercive force, but none having both a large B_r and H_c. Unless some special requirement dictates another material, an Alnico material more nearly meets the usual requirements. An added feature is that no material has a larger external energy product; hence, this group of magnets require less volume than other materials.

Commercially available are Alnicos 1, 2, 3, 4, 5 (several variations), 6, and 12. Of these, Alnico 2, 4, and 5 are available in the sintered state. Alnicos 5 and 6 are anisotropic, while the others are isotropic. The composition is 14-28% nickel, 0-25% cobalt, 8-12% aluminum, and sometimes plus a few percent of copper. The remainder is iron. Some have small amounts of additional elements such as titanium (5E) and columbium (5Cb). All of these magnets are hard and nonmachineable. They must be cast nearly to size, then ground to specifications. Alnico 12 is so brittle that it cannot even be ground. Bolt holes must be cored, or steel inserts placed in casting, which are later drilled and reamed.

The Alnicos (General Electric Company trade name) are practically nonaging with the passage of time, that is, the loss of magnetism is a few hundredths of one percent per century. For Alnico 5, the loss in remanance is 5% at 300°C, 12% at 500°C, and 100% at 900°C. Loss is

retraceable between - 200°C and 300°C, i.e., the loss at 300°C is regained when the temperature is lowered. Severe vibration may cause about 1% loss in remanance, but the effect is not cumulative though not retraceable. After a few impacts of the same amplitude, the loss ceases. The loss is due to the breakdown of feebly oriented molecular groups.

Figure 14 shows the demagnetization and external energy curves for several of the Alnicos. Alnico 5 possesses the highest B_r and B_dH_d, and thus was selected for use on this project. The coercive force is less than for Alnico 6 and 12. If the generator were to be subjected to severe demagnetization forces from current in the coil (related to armature reaction in rotating machinery), Alnico 6 or even Alnico 12 would be the better choice.

The composition of Alnico 5 is 24% cobalt, 14% nickel, 8% aluminum, 3% copper, and the remainder iron. The melt is poured in molds, and cooled in air from 1300°C in a magnetic field of 1000 to 3000 oersteds. The magnet is said to be anisotropic, that is, it must be magnetized in the same or opposite direction when in use as when heat treated in a magnetic field. Magnetization at right angles results in a loss of BH by a factor of 4 to 7. After cooling to room temperature, the magnets go through a hardening process by being baked at 600°C. This about doubles H_c, while B_r remains nearly constant. The physical basis of the high energy product and high anisotropy of Alnico 5 has not been established. Alnico 5 weighs 0.264 pounds per cubic inch (7.3 grams per cubic centimeter). It requires 3000 oersteds of magnetizing force per centimeter of length of magnet to magnetize in customer's assembly.

Consideration of Figure 15, shows that a good material for the yoke and front plate would be type "4750", 48% nickel and the rest iron. The

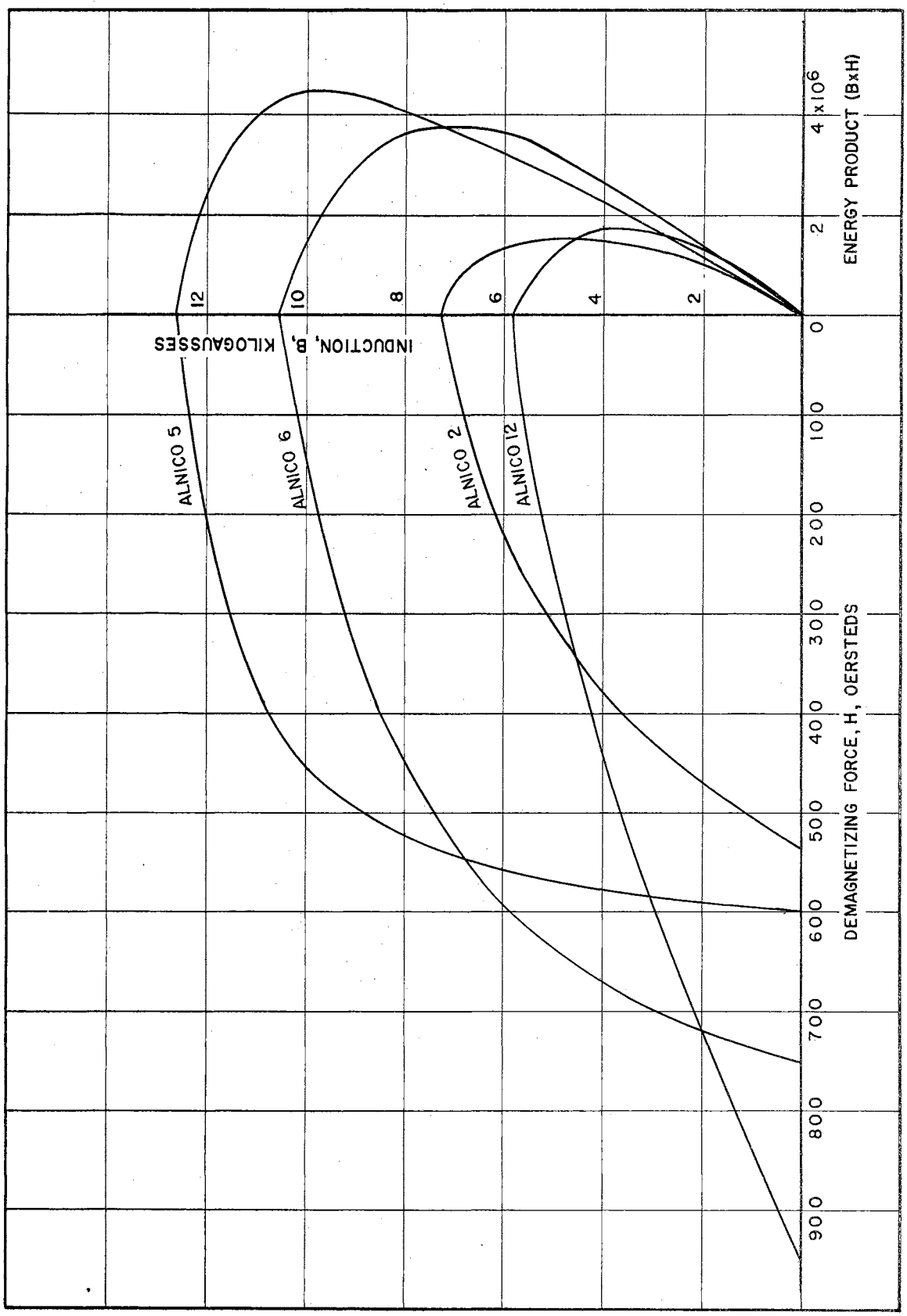

Figure 14. Demagnetization and External Energy Curves for Part of the Alnico Group.

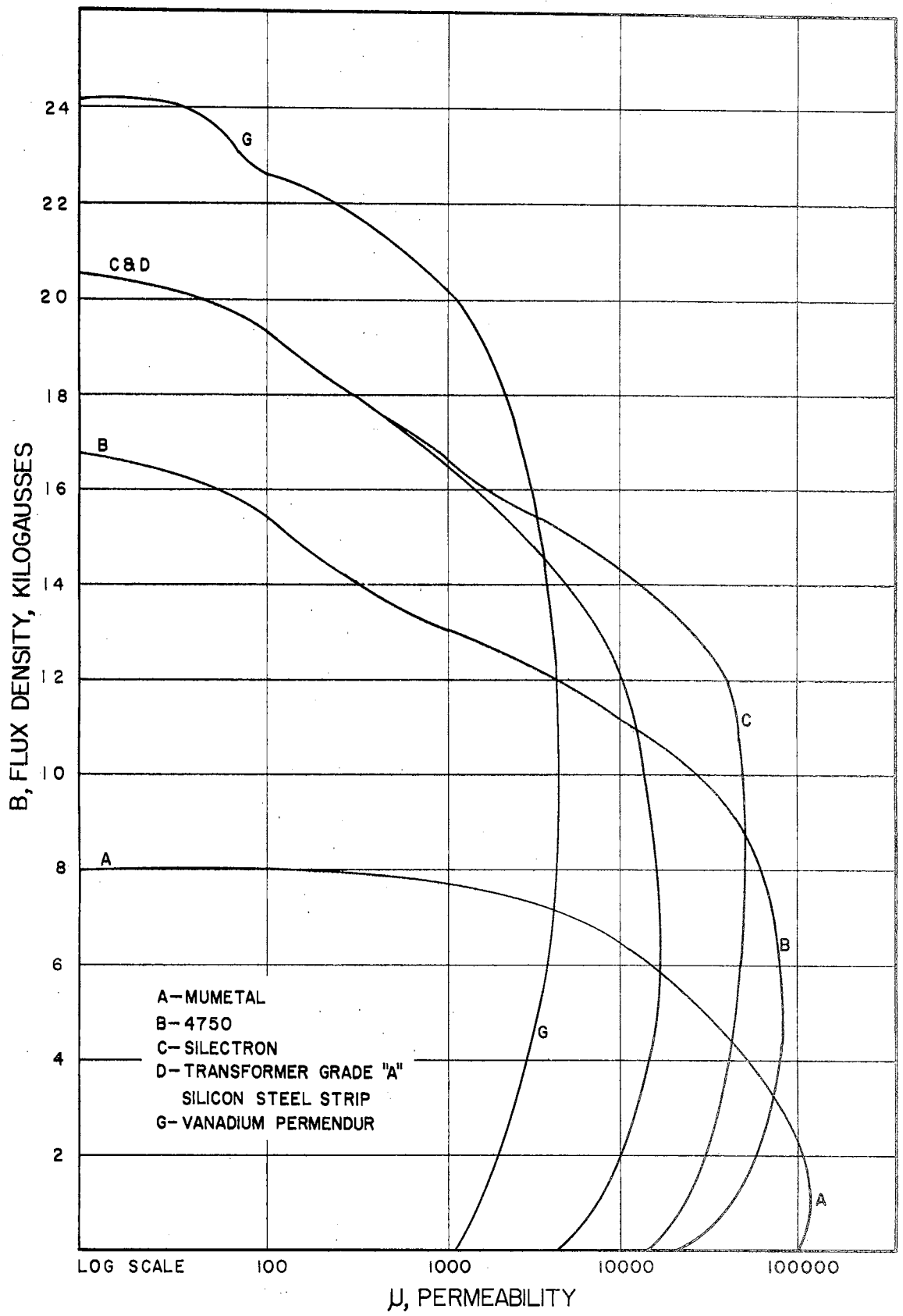

Figure 15. Permeability Curves for Magnetic Core Materials (Allegheny Ludlum Steel Corp.).

cross-sectional area of these parts should be designed for 6 kilogausses. The pole piece must carry considerably more flux so that Silectron would be more suitable than "4750." Unfortunately, the manufacturer could not supply these materials in the sizes desired.

It was once thought that a $\frac{1}{2}$-inch long, $\frac{1}{4}$-inch deep notch in the pole piece just inside the air gap would cause more flux to pass through the air gap. Further consideration revealed that the notch would cause excessive flux saturation in the pole piece.

There are many materials with high magnetic permeability. However, this maximum may occur at a low value of flux, or may be a very sharp curve so that maximum permeability would be realized only at a very small band of flux densities, and some are obtained only for a fraction of a second. Some of the materials are so special as to be unobtainable at even high cost. One promising material is Permendur (50% cobalt), which has a maximum permeability of 5000 at 12 kilogausses with saturation occuring at 24.5 kilogausses. This material might be used for the front plate (to reduce thickness and increase B_g) and for the pole piece which, at 1.5-inch diameter, appears to be critical. After a material reaches saturation it might as well be air or any other nonmagnetic material. The silicon-irons would be acceptable materials. Four per cent silicon-iron has μ_m = 10,000 at 7 kilogausses, with saturation occuring at 19.7 kilogausses.

It was desirable to obtain a material in 5, 2 and 5/8-inch rounds, the 5/8 round sample being used to obtain a virgin magnetization curve and hysteresis loop.

The only material readily available with these dimensions was American Iron and Steel Institute (AISI) C-1018 mild, hot-rolled steel. This

was not an electrical grade, but to gain considerable time this material was used after experimental saturation curves revealed that it was acceptable. The AISI C-1018 (also SAE 1018) steel has the following composition as given by the manufacturer: 0.15/0.20% carbon, 0.6/0.9% manganese, 0.04% maximum of phosphorus, and 0.05% maximum of sulphur. It is weldable, weighs 2.67 pounds per foot of 1-inch round, is hot rolled from open hearth steel, and may be full-annealed at 1550-1650°F, then cooled in the furnace.

The magnetization curves (permeability curves calculated therefrom), in the as-received state and after annealing, are shown in Figure 16. The hysteresis loop for the sample in the annealed state is shown in Figure 17. These data were obtained with a number 2239-E, Leeds & Northrup ballistic galvanometer, with a circuit similar to that shown in American Society for Testing Materials (ASTM)[21] designation A341-55. It may be noted from Figure 16 that the flux density at which maximum permeability occurs is down slightly after annealing, but that the permeability is increased from 670 to 810 or about a 21% increase. The hysteresis loop in Figure 17 is thin, a characteristic of soft ferromagnetic materials. The extra thin tips indicate that the material was carried considerably beyond saturation. The remanance is approximately six kilogausses. This might be thought to be aiding the permanent magnet, but measurements with the gaussmeter (without a permanent magnet in the circuit) indicated less than 200 gausses in the air gap.

With the curves of essential properties of Alnico 5 and of the yoke material, the design of the magnetic circuit was undertaken.

---

[21] Standard Methods of Test for Normal Induction and Hysteresis of Magnetic Materials, (American Society for Testing Materials, Philadelphia, 1955), p. 1444.

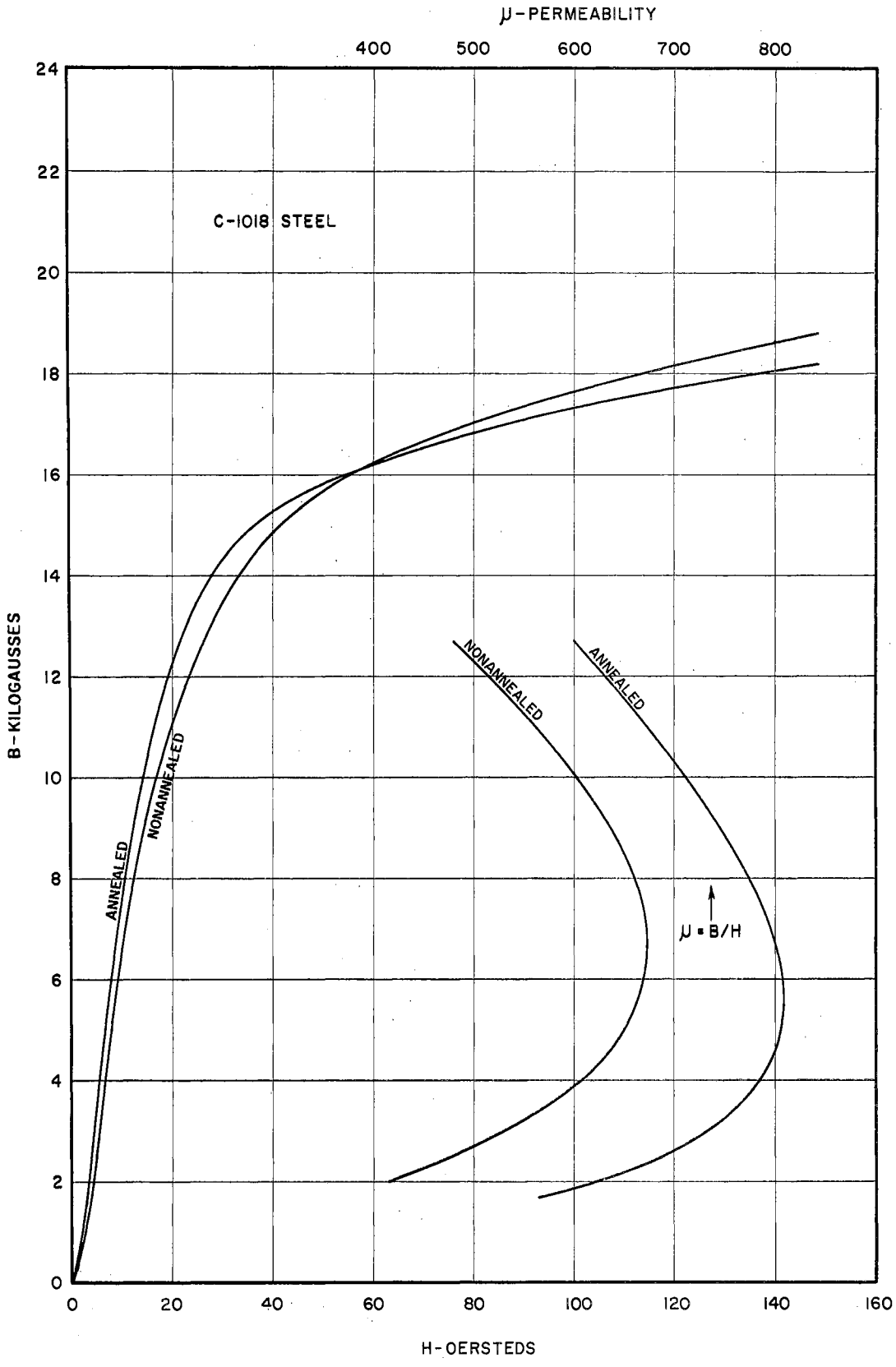

Figure 16. Magnetization and Permeability Curves, C-1018 Steel.

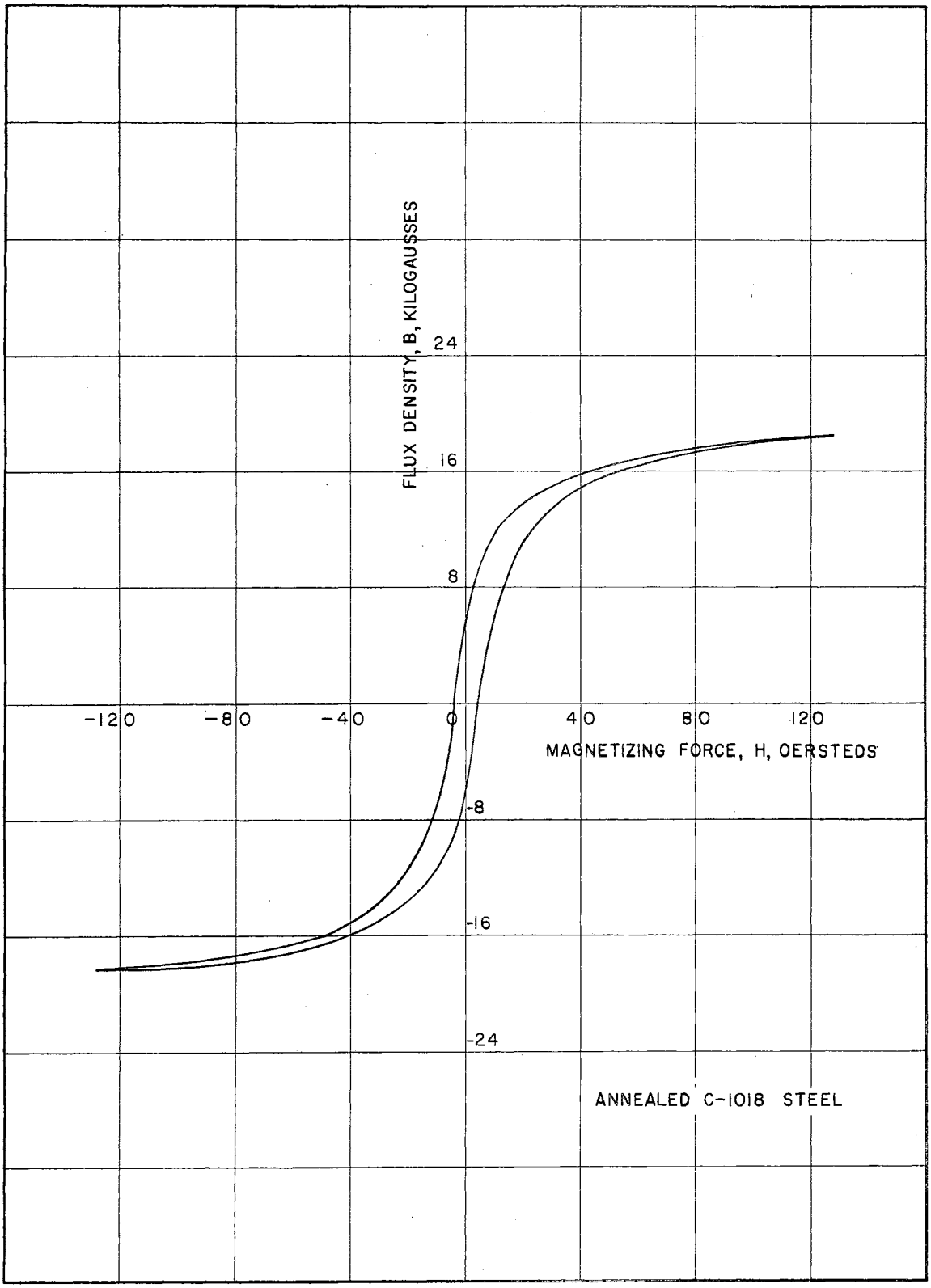

Figure 17. Hysteresis Loop for Annealed C-1018 Steel.

A pole piece radius of r = 1.905 cm (1.5-inch diameter) and the radius to the center of the air gap, R = 2.095 cm, were assumed for leakage flux calculations. The air gap length, L_g, was 0.381 cm, the difference in diameters divided by two, where the diameter of the hole in the front plate was 4.572 cm (1.8-inch diameter).

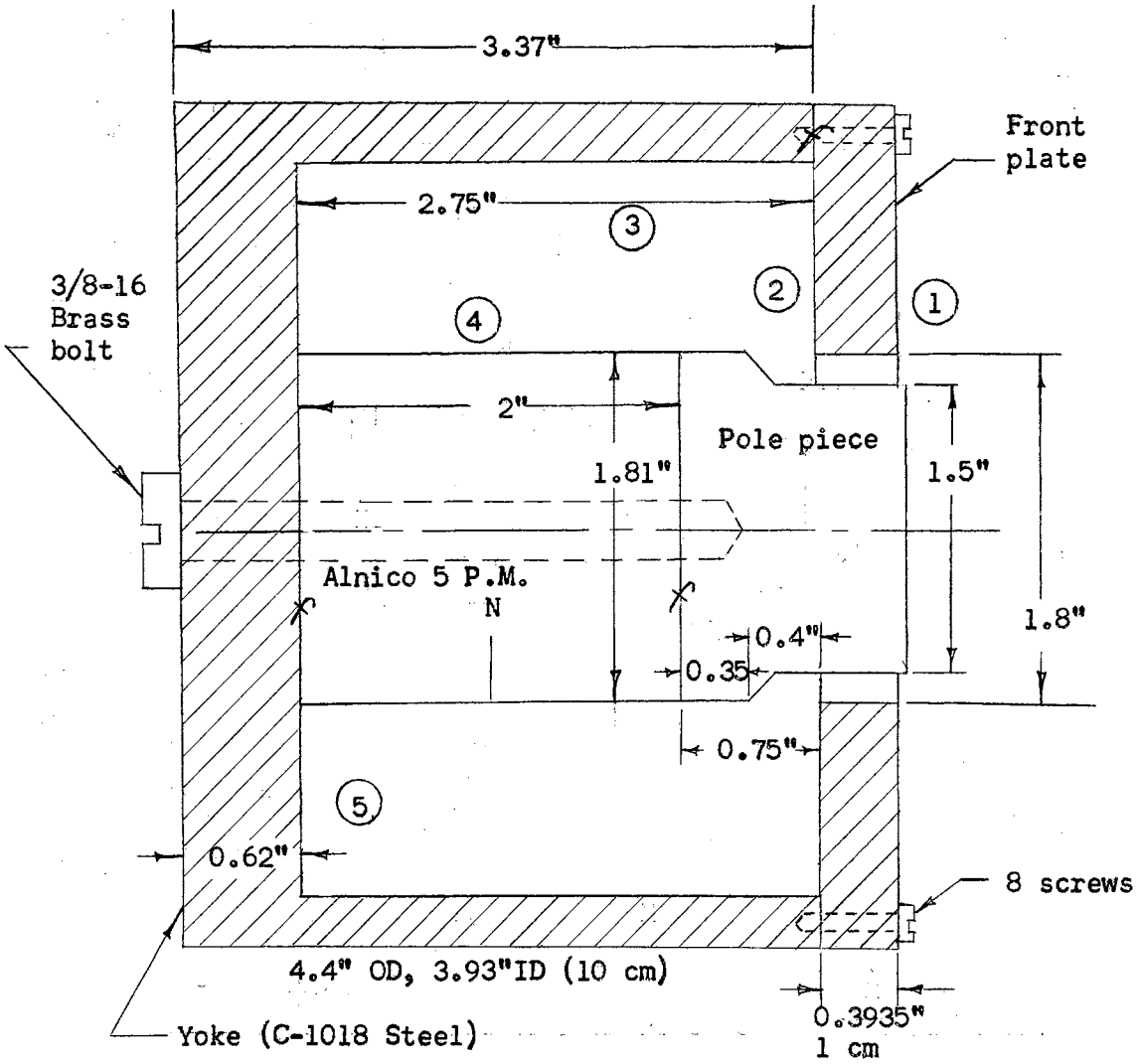

Figure 18. Cross section of generator number one.

As an initial value, to ascertain the leakage factor, F, the design was based on 4200 gausses in the air gap. Along the pole piece, A_g = 2πrdepth = 6.28 x 1.905 x 1 cm = 11.96 $cm.^2$

$\phi = B_g A_g = 4200 \times 11.96 = 50{,}250$ lines.

$H_g L_g = B_g L_g = 4200 \times 0.381 = 1600$ gilberts.

For calculation of leakage flux the usual assumption was made that the reluctance drops in the iron and the joints were small enough to neglect.

The area one leakage flux was 58% of the air gap flux from page 34.

$\phi_1 = 50{,}250 \times 0.58 = 29{,}150$ lines.

Area two reluctance was $\mathcal{R}_2 = \frac{\pi}{4[\pi r \ln t/L + 2(t - L)]}$ from equation (20). This was modified by a factor of 0.87 from page 35. A decrease in dimension t would increase $\mathcal{R}$ and thus reduce the leakage flux. However, sufficient space must be allowed for the magnetizing winding. Let t = 2 - $\frac{1}{2}$D of pole piece = 2 - 0.75 = 1.25 inches or 3.175 cm.

$$\mathcal{R}_2 = \frac{\pi}{4[\pi\, 1.905 \ln 3.175/0.381 + 2(3.175 - 0.381)]} = 0.043 \text{ units.}$$

$\phi_2 = MMF/\mathcal{R} = 1600/0.043 = 37{,}200$ lines.

Corrected $\phi_2 = 37{,}200/0.87 = 42{,}750$ lines.

The reluctance of the radial leakage path (area three) was $\mathcal{R}_3 = \frac{\ln[(t + r)/(r)]}{2\pi h}$ from equation (21). A reduction in h would increase $\mathcal{R}$, and thus reduce the leakage flux. Let h = 1.905 cm (0.75 inches) for the pole piece. One-half of magnet length was estimated as 2.54 cm (1 inch). For the purpose at hand the magnet diameter was assumed to be the same as the pole piece (1.5 inches). Total h = 1.905 + 2.54 = 4.445 cm.

$$\mathcal{R}_3 = \frac{\ln\left(\frac{3.175 + 1.905}{1.905}\right)}{2\pi\, 4.445} = 0.0352 \text{ units.}$$

$$\phi_3 = \frac{1600/2}{0.0352} = 800/0.0352 = 22{,}700 \text{ lines.}$$

Area five reluctance required the area two formula modified in that

L = 2.54 cm, with t = 3.175 as before.

$$\mathcal{R}_5 = \frac{\pi}{4[\pi r \ln t/L + 2(t - L)]} = \frac{0.7854}{\pi 1.905 \ln 3.175/2.54 + 2(3.175-2.54)}$$

= 0.3015 units.

ϕ_5 = 1600/0.3015 = 5310 lines.

Corrected ϕ_5 = 5310/0.87 = 6110 lines.

As this value was small, the overall result will not be changed appreciably if the magnet diameter were not as assumed.

The summation of gap flux and the leakage fluxes for areas 1, 2, 3, and 5 was 150,960 lines. Allowing for magnet surface leakage (area four) by division by 0.93 (see page 37):

ϕ_t = 150,960/0.93 = 162,400 lines. This was the total flux passing through the neutral section of the magnet. The surface leakage flux was 11,440 lines.

The leakage factor, F = 162,400/50,250 = 3.23. Small f = 1.1 from page 38.

For readers with a knowledge of fields, it must be realized that exact field theory will, in the simplest cases, be too cumbersome to apply, and, in general, the complexity of the boundary conditions and the multiple-functioned relation of B and H render a mathematical solution hopelessly complicated. Furthermore, variations in magnetic quality of material among magnets and in the same magnet make exact calculations futile from a practical standpoint. Leakage flux calculation is like solving an electrical circuit for current in metallic conductors immersed in salt water.

Referring to Figure 19, it may be seen that for a static design, the operating point would be chosen at B_d = 9 kilogausses where the energy

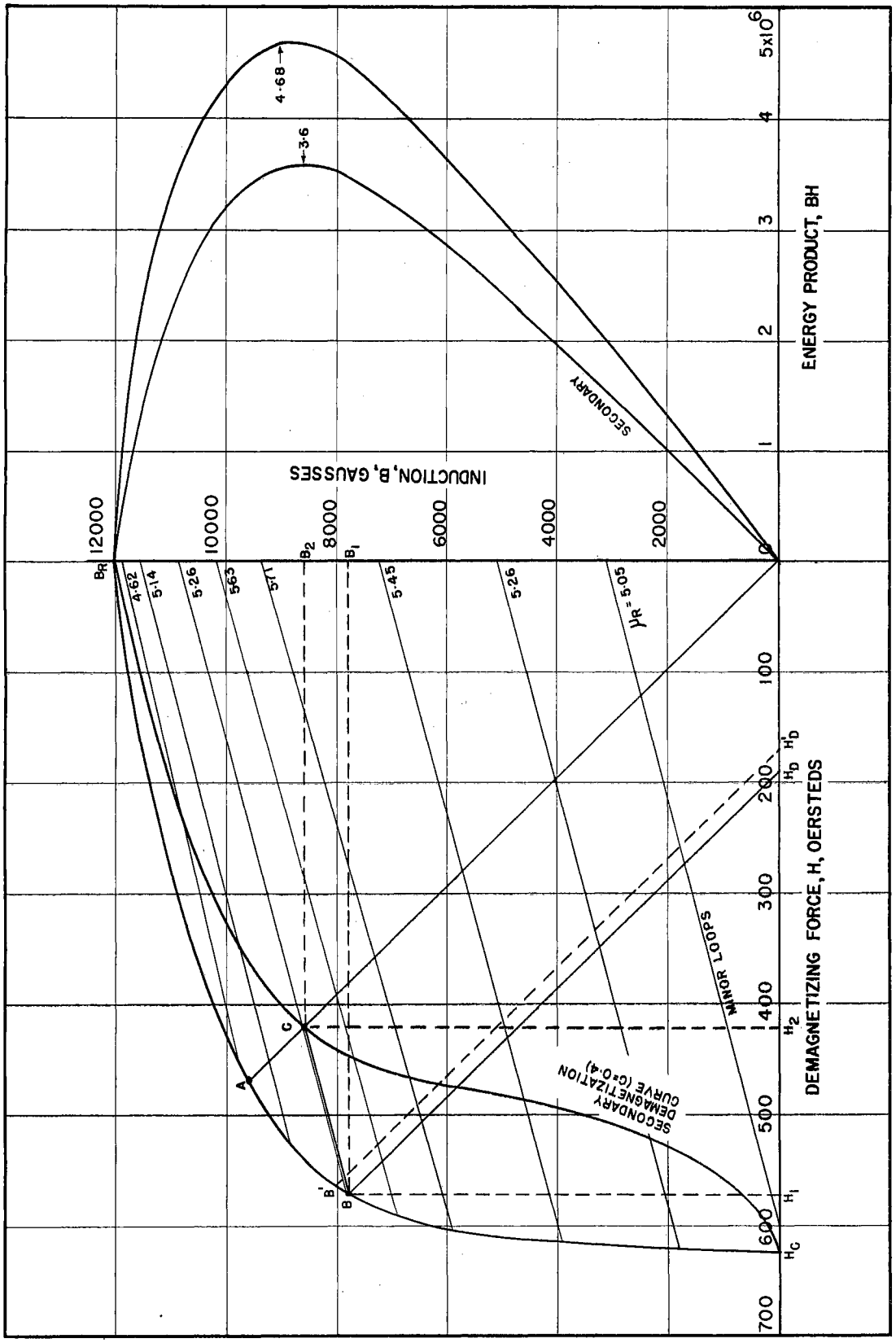

Figure 19. Alnico 5 Demagnetization Curve with Minor Loops (Arnold Engineering Company); Secondary Demagnetization and Energy Product Curves.

product is a maximum at 4.68×10^6. However, some stabilization of the magnet was desired. After demagnetization and recoil along a minor loop, the regular demagnetization curve cannot be used to calculate the energy product curve. For a given stabilization with a reverse MMF, the problem was to derive a secondary demagnetization curve for which all points on this curve would provide the same amount of stability. The operating point should be located on the secondary demagnetization curve opposite the maximum point of the secondary BH_{max} point on the energy product curve.

A method of calculating this secondary demagnetization curve from the major demagnetization curve has been provided by Cioffi.[22]

The demagnetization force, F_d, is $H_d L_m$, while the operating MMF (or F) is $H_2 L_m$. Refer to Figure 19 to locate these points. To establish B-H_d, draw B-H_d parallel to AO, the air-gap line. L_m, the length of the magnet, is not yet known, but define a factor,

$$C = F_d/F = H_d L_m / H_2 L_m = H_d/H_2. \tag{25}$$

By definition, the reversible permeability, $\mu_r = \dfrac{(B_2 - B_1)}{(H_1 - H_2)}$ (26)

The slope of OA, $S_2 = B_2/H_2 = B_1/(H_1 - H_d)$. (27)

The simultaneous solution of these equations yields,

$$H_2 = \frac{(B_1 + \mu_r H_1)\left[(c + 1) - \sqrt{(c + 1)^2 - 4\mu_r c H_1/(B_1 + \mu_r H_1)}\right]}{2\mu_r c} \tag{28}$$

From (26), $B_2 = \mu_r(H_1 - H_2) + B_1$. (29)

For a given $c = H_d/H_2$, points B_1 and H_1 on the demagnetization curve may be assumed, and points on the secondary demagnetization curve calculated with equations (28) and (29). B_r, H_c, and the operating point (C in

---

[22] P. P. Cioffi, "Stabilized Permanent Magnets," Transactions of the AIEE, Vol. 67, Part II, (New York, 1948), pp. 1540-1543.

Figure 19) will be on this curve. With values on this curve, the secondary energy product curve may be calculated. While a family of such curves could be plotted, a value of $c = H_d/H_2 = 0.4$ was assumed. One calculation only will be shown, with the complete data plotted in Figure 19.

Using $c = 0.4$, $\mu_r = 4.62$, $B_1 = 9800$, $H_1 = 450$,

$$H_2 = \frac{(9800 \neq 4.62 \times 450)}{(0.4 \times 2 \times 4.62)} \left[1.4 - \sqrt{1.96 - \frac{4 \times 0.4 \times 4.62 \times 450}{9800 \neq 2080}}\right]$$

$$= \frac{(11,880)}{(3.69)} \left[1.4 - \sqrt{1.96 - 3325/11,880}\right] = 3220 \left[1.4 - \sqrt{1.96 - 0.28}\right]$$

$$= 3220 \left[1.4 - \sqrt{1.68}\right] = 3220(1.4 - 1.3 = 3220 \times 0.1$$

$$= 322 \text{ oersteds.}$$

$$B_2 = 4.62(450 - 322) \neq 9800 = 4.62 \times 128 \neq 9800 = 592 \neq 9800$$

$$= 10,392 \text{ gausses.}$$

The maximum point on the new BH curve occurred at 3.6×10^6, hence the operating point C was located on the secondary demagnetization curve. This automatically located point A on the major demagnetization curve before stabilization. Since $c = 0.4$ was selected, $H_d = 0.4H_2 = 0.4 \times 418 = 170$. Point B was then located. For the minor loop to pass through point C, $H_d = 190$ instead of 170 had to be used. This amounted to an error of 20 oersteds or 11.75%, due to inaccuracies in calculations and plotting.

The remainder of the magnet design consisted of selecting a B_g, calculating magnet dimensions to produce a static design at point A, after which a demagnetizing force of 190 oersteds will be applied to move the point along the major curve to point B. Removal of this force allows the operating point to move to the desired point C as a stable operating point so long as any future demagnetizing force is 190 oersteds or less. Within this range the minor loop is reversible.

The overall design efficiency, $B_2H_2/(BH)_{max}F = 3.6x10^6/(4.68x10^6x3.23)$ = 3.6/15.12 = 23.8%, represents the optimum obtainable under the imposed conditions. The difference between 4.68 and 3.6 is the price paid for stabilization.

Equation (23): $L_m = \frac{fB_gL_g}{H_m} = \frac{1.1 \times 4200 \times 0.381}{468}$

= 3.76 cm or 1.48 inches, assuming that an air-gap flux density of 4200 gausses was desired.

Equation (24): $A_m = \frac{FB_gA_g}{B_m} = \frac{3.23 \times 4200 \times 11.96}{9620}$

= 16.87 cm. To this was added the 0.713 cm^2 area of the bolt hole, so that A_m = 17.583 $cm.^2$ From $A = \pi/4\ D^2$, $D_m = \sqrt{4A/\pi} = \sqrt{4 \times 17.583/\pi} = \sqrt{22.35}$ = 4.73 cm or 1.863 inches.

The Alnico 5 magnet should be 1.863 inches, outside diameter, 0.375 inches, inside diameter, and be 1.48 inches in length. Only the Arnold Engineering Company, Marengo, Illinois, of five companies queried, could come close to these specifications. The magnet, as available, 1.81250D, 0.375ID x 1.5 inches long, was ordered from this company. The effect of the difference of 0.0505 in D_m and 0.02 inches in L_m was thought to be negligible. Of course, a magnet of design dimensions could be ordered at a total cost of about $100, including the cost of a temporary pattern, but delivery would be uncertain at about two months. Most manufacturers do not wish to be bothered with small orders.

This magnet has been designed a number of times. Slightly different values of f and F, and use of curves from different manufacturers, and various assumptions will produce any number of slightly different values. Further refinement of design would require many models. This would not

be economically justifiable at this stage of development.

After stabilization to point C where B_d = 8.6 kilogausses, H_2 = 418, the air gap flux density will be, from equation (24),

$$B_g = \frac{A_m B_d}{F\ A_g} = \frac{16.87 \times 8600}{3.23 \times 11.96} = 145{,}000/38.65 = 3750 \text{ gausses.}$$

For the design of the iron portions of the magnetic circuit, it was convenient to tabulate the various fluxes, giving the percent of the total flux through magnet neutral.

ϕ_g	= 50,250 lines	or 30.93% of ϕ_t
ϕ_1	= 29,150	17.94%
ϕ_2	= 42,750	26.33%
ϕ_3	= 22,700	13.98%
ϕ_4	= 11,440	7.05%
ϕ_5	= 6,110	3.77%
ϕ_t	=162,400	100.00%

Consideration of ϕ in pole piece near magnet:

By ratio of lengths, 0.75/1.75 x ϕ_3 = 0.42 x 22,700 = 9730 lines. Total pole piece flux was part ϕ_3, found above, + ϕ_g + ϕ_1 + ϕ_2 = 9730 + 50,250 + 29,150 + 42,750 = 131,880 lines. The area of the pole piece was $\pi/4\ (1.81)^2$ = 0.7854 x 3.27 = 2.57 in.^{2} or 16.58 cm.^{2}

$B_{pp} = \phi/A$ = 131.88/16.58 = 7.95 kilogausses.

Permeability is 775 from the annealed curve in Figure 16 as compared with the maximum of 810.

Consideration of ϕ in pole piece just before the diameter changes from 1.5 in. to 1.81 in:

By ratio again, radial ϕ_3 was 0.4/1.75 x 22,700 = 5190 lines.

Area two $R_2 = \frac{\pi}{4[\pi r \ln t/L + 2(t - L)]}$ where t was 0.4 inches or 1.015 cm. This calculation yielded a reluctance of 0.1102 units.

ϕ_2 = 1600/0.1102 = 14,520 lines.

Corrected ϕ_2 = 14,520/0.87 = 16,680 lines.

The summation of flux through this area was $\phi_1 + \phi_g + \phi_2 + \phi_3$ or 101,270 lines. The pole piece area here was 1.77 in.^{2} or 11.4 cm.^{2}

$B_{pp} = \phi/A = 101.27/11.4 = 8.88$ kilogausses. From Figure 16 the permeability is 745. The pole piece was annealed because of this critical area.

Consideration of the ϕ through the air gap on the surface of the front plate:

The flux density in this region on the pole piece has been assumed as 4200 gausses. Hence, the flux density on the surface of the front plate over the air gap will be lower because of the greater surface area. This material was not annealed (only the critical item, the pole piece, was annealed) and further, some hardening and consequent loss in permeability due to machining stresses may be expected.

Consideration of the back plate surface area as if there were a hole of the same diameter as the magnet: this area was π D x depth = π 1.81d = 5.68d or 14.43d using centimeters. This section carried all of the operating flux except the surface leakage, namely 150,960 lines.

$B = \phi/A = 150.96/14.43d$; $d = 150.96/14.43B$. Selection of B = 6.63 kilogausses was made. Then $d = 150.96/(14.43 \times 6.63) = \frac{150.96}{95.6} = 1.573$ cm or 0.62 inches. $A = 14.43 \times 1.573 = 22.7$ cm^2.

The dimensions of the generator in Figure 18 were shown in inches for the convenience of the machinist.

The area of the yoke just forward of the back plate (back plate was integral with the yoke in this design to eliminate the air film reluctance drop) will carry all of the flux except surface leakage, and area five leakage flux, namely, 150,960 - 6110 = 144,850 lines. Selection of B = 7.18 kilogausses was made.

$\phi/B = A = 144.85/7.18 = 20.15$ cm^2 or 3.13 in^2.

$A = \pi/4\ (D_2^2 - D_1^2)$. D_1 was fixed at 3.93 in.

$3.13 = 0.7854(D_2^2 - 15.4)$

$3.99 = D_2^2 - 15.4$ (See Figure 20)

Whence, $D_2^2 = 15.4 + 3.99 = 19.39$; $D_2 = 4.4$ inches.

The wall thickness was $(D_2 - D_1)/2 = 0.47/2 = 0.235$ inches.

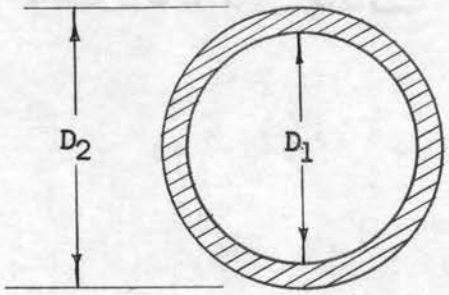

Figure 20.

Probably no areas will operate at the maximum permeability (for lowest reluctance drop obtainable with the material used), but extraordinary low permeability has been avoided as well as saturation. For example, a B_m of 16.5 kilogausses will be required to saturate the magnet in the assembly in order to obtain the B_r of 12.0 kilogausses listed by the manufacturer. Magnet flux will be 16.5 x 16.87 = 278.5 kilolines during the magnetization process. About 93% of this, or about 258.5 kilolines, will be in the back plate area next to the magnet.

$B = 258.5/22.7 = 11.39$ kilogausses.

This is still below the saturation region where the magnetization curve in Figure 16 assumes a constant slope. This is also true of the other critical areas since they were calculated by ratio.

When the Alnico 5 permanent magent was received from the manufacturer it was lapped for smoothness and inserted into the yoke. The length was

1.45 inches instead of the design value of 1.48 inches. Also, the hole in the magnet was 0.3435 inches instead of 0.375 inches. The raised shoulder of the pole piece was 0.72 inches, and the 1.5-inch diameter portion was 1.03 inches in length. The overall length of the pole piece was thus 1.75 inches. The dimensions shown on Figure 18 were altered to this extent.

Three hundred turns of number 14, heavy formex-insulated, copper wire were wound on the magnet and pole piece shoulder as a magnetizing winding. The assembly was magnetized with 52.5 amperes so that the applied MMF was 15,750 ampere-turns. With the light-beam flux meter and a one-turn search coil the flux density in the air gap was found to be 4400 gausses as compared with the design value of 4200 gausses. The difference was 200 gausses or 4.76%. Considering the many variables, this was quite fortuitous.

It was evident that one-half inch could be removed from the axial length of the yoke to improve the design. However, the extra length was retained, and 0.56 inches of additional permanent magnet was added so that the total magnet length was 2.01 inches. In testing the generator by vibrating the coil in the air gap flux there was more interest in a high flux density than in the optimum design to minimize the magnet material. The shorter pole piece had a raised shoulder of 0.43 inches length, 0.75 inches length of the 1.5-inch diameter portion, with the overall length being 1.18 inches. The changes in pole piece and magnet lengths were the only deviations from the dimensions shown in Figure 18. This assembly, which was identified as model two, was magnetized with 50 amperes or 15,000 ampere-turns of MMF. The hand gaussmeter read 5.1 kilogausses while the pull-off coil method gave 5.06 kilogausses in the air gap. For convenience, the demagnetization was effected by using 3 amperes in the magnetizing

coil without closing the air gap. Flux density in the air gap was reduced to 4800 gausses. This indicated that the demagnetizing influence of current in the armature coil would not be appreciable.

An exploded view of generator number one is shown in Plate I. A photograph of the assembled generator number two is shown in Plate II.

Plate I

Exploded View of Generator Number One

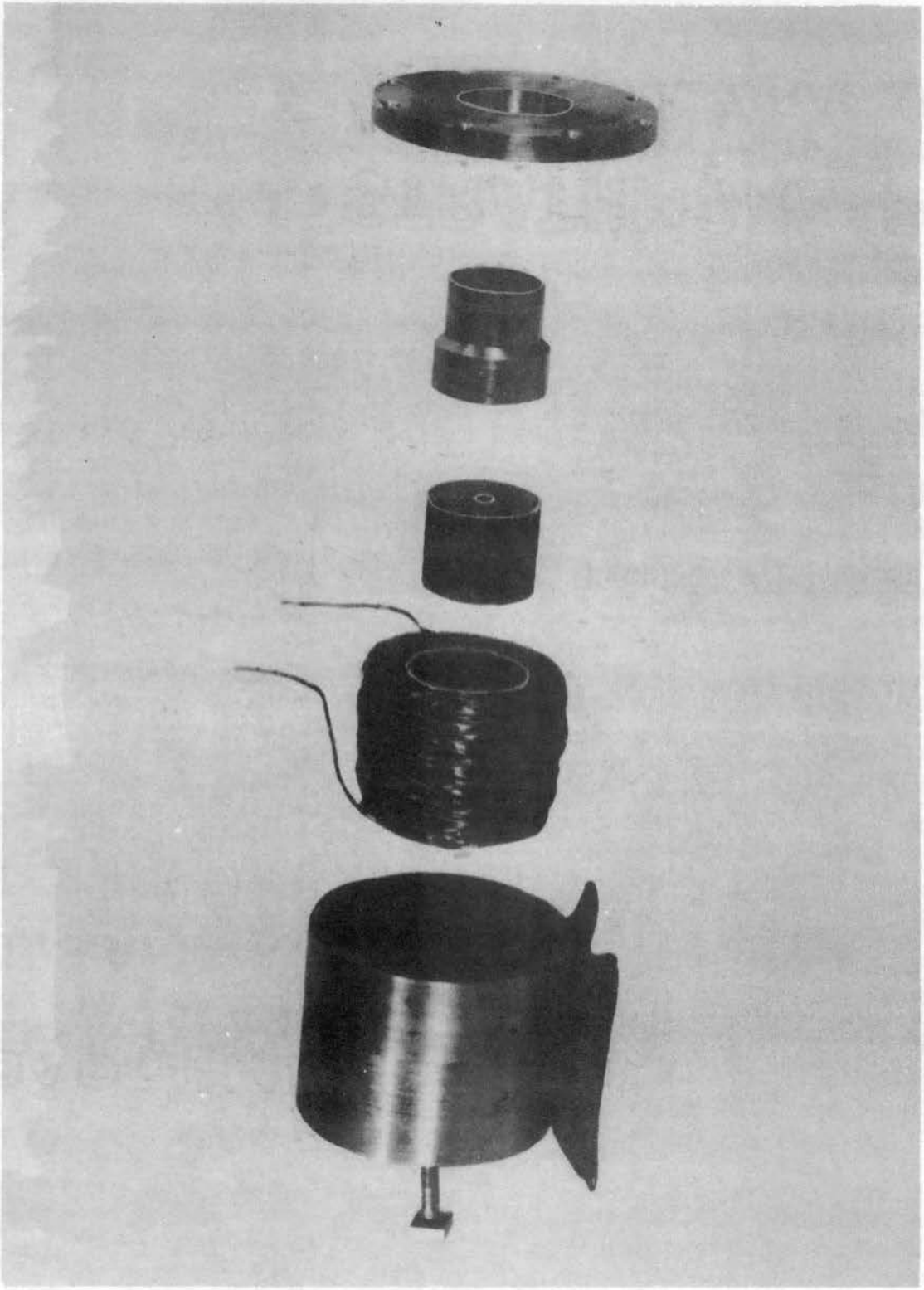

Plate II

Assembled View of Generator Number Two

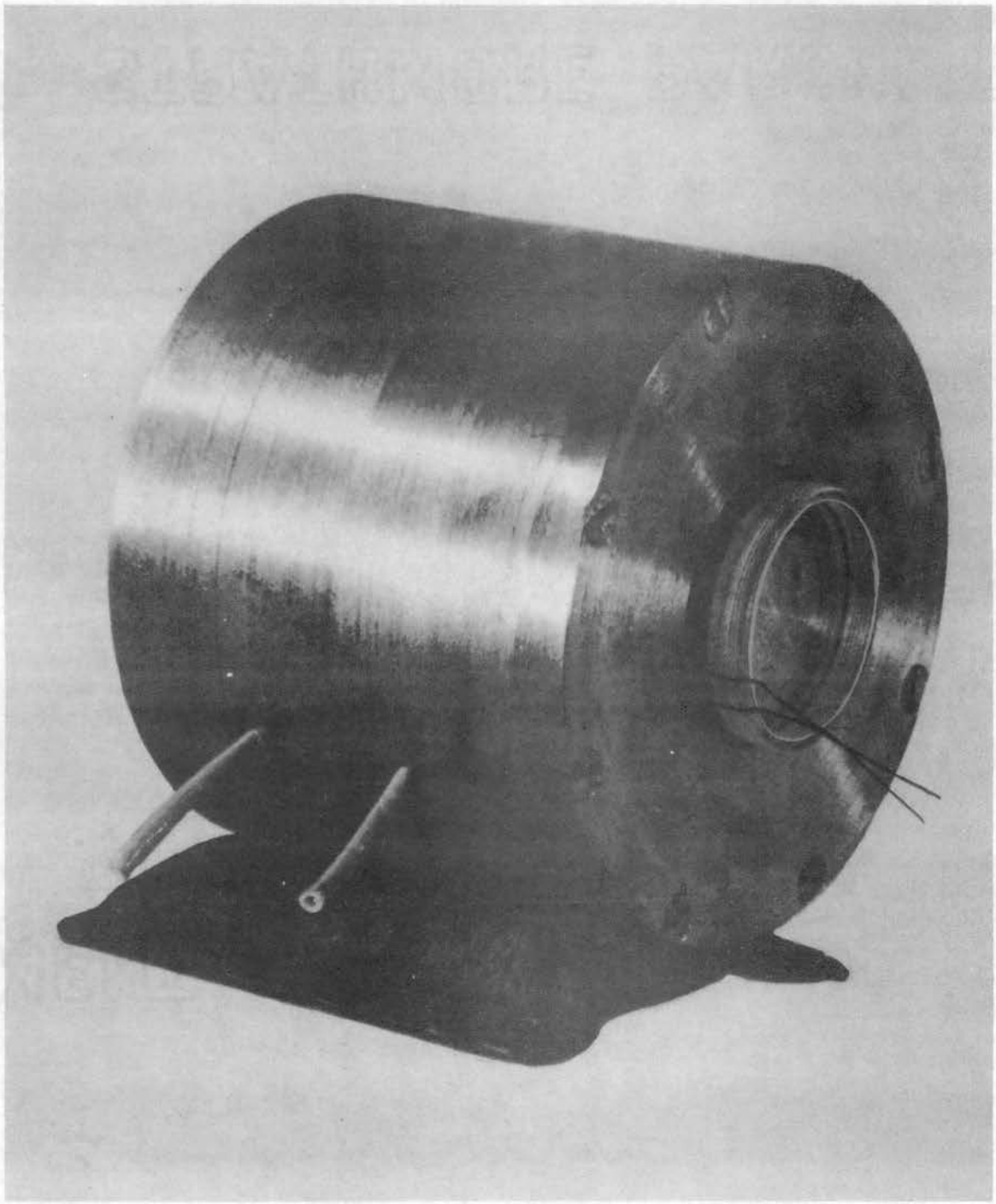

CHAPTER VI

COIL AND COIL FRAME DESIGN

The coil will of necessity have to be cylindrical. It should not rub on the pole piece or face plate as undesirable friction and possible damage would result.

When current flows in the coil a flux will pass through the coil. There will be a north magnetic pole (equivalent) where the flux leaves the coil, and a south pole where the flux enters. Since the coil lies between north and south magnetic poles due to the PM_g some attraction and repulsion will result. The magnitude of this turning force will be a function of the load current. Large currents might produce sufficient turning force to cause undesirable coil frame rubbing. However, large currents will not occur, even on short circuit.

The MMF causing the coil flux is $0.4\pi NI$ gilberts. The coil flux will be either aiding or bucking the flux provided by the permanent magnet. The bucking portion will be manifested as a demagnetizing force. The aiding portion should not move the operating point along the recoil line much beyond the $H = 0$ line or the magnet will be remagnetized slightly to cause operation along a new recoil line. The effect on the permanent magnet assembly of this alternating demagnetizing and magnetizing is similar to armature reaction in rotating dynamos.

It is not possible to use two coils on the coil frame of opposite winding sense with the idea of having fluxes from each cancelling because

induced voltages will drive a current in each in such direction that the fluxes will always be aiding.

It is desirable to have a low impedance in the coil. Low resistance means low heat loss from I^2R, and also insures a good regulation. As the load current goes up, the generated voltage is dropped in the coil and in the load. A low resistance means that less of the generated voltage is dropped in the coil so that a major part is available for the load. A high resistance and consequent high I^2R in the coil might produce sufficient heat in the coil to destroy the insulation varnish on the wire or to melt or deform the frame material.

As the coil oscillates in the air gap, air resistance may be appreciable. This can be ascertained by test.

The copper wire on the frame will be subjected to a force, $F = BLI$, tending to force the wire off of the frame. The input force, F_i, will be larger than BLI by other losses such as rubbing friction loss, air resistance, eddy current, hysteresis loss, etc. The wire should be tightly wound and cemented in place. Holding nibs should be provided on the coil frame. An extreme remedy would be to cast the coil in say, lucite plastic. Should the added strength of an aluminum frame be necessary, excessive eddy current loss will probably occur.

The velocity input, ideally, should be a sine wave so that a voltage wave of like shape will be generated. Circuit calculations are simplified when voltage and current are sine waves. Substantial deviation from the ideal necessitates the use of the Fourier Series method involving considerable calculation. A peaked wave current could be rectified, and used to charge a capacitor from which some d.c. power could be drawn.

A low self-inductance in the coil is desirable to keep the coil

impedance low. In an air core coil where all of the flux links all of the turns, the self-inductance is loosely defined as $L = N\phi/I\ 10^{-8}$ henrys, with ϕ in lines and I in practical amperes. A more rigorous definition is $L = N\ d\phi/di\ 10^{-8}$ henrys. (30)

Inductance is a property that opposes any change in the current. It may be compared with inertia in a mechanical system. When iron is present, L becomes a variable as a function of current. A system is linear if the magnetic potential drop in the ferrous parts of the system is negligible. Then $L = N\phi/I$ might be used if all of the coil flux links all of the turns.

Total coil displacement was selected as 0.1-inch (0.254 cm). The face plate air gap axial length was set at one centimeter. If the coil vibrates 0.127 cm in each direction from a midpoint, the coil width must be such that none of the coil turns will be beyond the air gap area. Should any turns of the coil have motion outside of the constant flux density area, the voltage wave shape would be adversely affected.

Originally, a weight of 20 grams was alloted to the coil and coil frame. Any reduction would aid the prime mover.

While long life and reliability are desirable characteristics of the coil assembly, they are not of prime importance in the development stage. As will be apparent in the prime mover design chapter, ability to withstand shock is one of the more important requirements.

Materials for the coil frame might be aluminum, fibreglass, lucite, micarta or nylon. As a beginning, cast lucite plastic, 1.75-inch OD, 1/8-inch wall thickness, before machining, was selected on the basis of availability and apparent suitability. The frame was polished after machining to remove tool marks to reduce the possibility of breakage. From Figure 21, it can be seen that the coil winding space is 3/16-inch

by 1/32-inch deep.

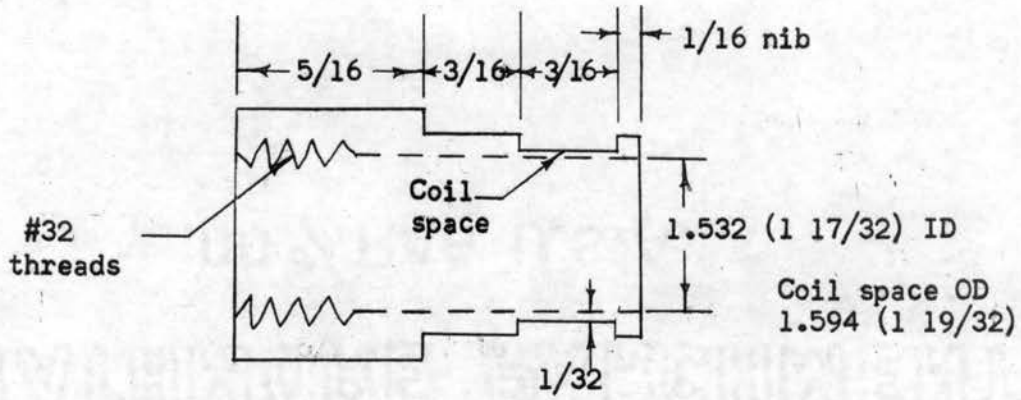

Figure 21. Cast lucite coil frame with dimensions in inches. (Not drawn to scale)

A short length of low-resistance large-diameter wire could be wound on the frame, or a long length of high-resistance small-diameter wire might be used. As a compromise about 30 feet (915 cm, 76 turns) of #30 varnish-insulated copper wire was wound in the coil space. The weight of the frame was 5 grams, and that of the wire 4 grams, or a total of 9 grams of weight to be oscillated in the air gap. The Kelvin double bridge resistance measurement was 3.55 ohms at room temperature. Although not reliable, the Heath-kit bridge measurements of inductance were 0.38 millihenrys (mh) with the coil out of the generator frame, and 0.62 mh with the coil in the iron frame (i.e., inserted in the air gap). The self-inductance appeared to be negligible.

With the coil in the gap, one ampere of 60 cps current at 3.6 volts was sent through the coil. A wattmeter read 3.8 watts. This indicated that the impedance was mostly resistive with little inductance, but the wattmeter reading at such a low value is not accurate. The current was set at one ampere with the coil out. The current dropped to 0.99 amperes when the coil was inserted in the air gap. On this basis, L would be

equal to about one millihenry. When 1000 cps was used, there was no change in the ammeter current whether the coil was in the frame or out. The overall survey of inductance seemed to indicate that it was small.

When the coil was allowed to vibrate, the amplitude of vibration was very small at 1000 cps, but quite large at 60 cps.

As a side light, a split brass hollow cylinder with input wires on either side of the split was tried as a combination coil and frame. The cylinder was insulated with electrical scotch tape. The inertia was so great as to prevent vibration altogether.

Equation (5) states that $e = BLv\ 10^{-8}$ volts, where L is the length of wire instead of N turns x average length of one turn. B is in gausses, L in centimeters, v in cm/sec., and e in volts. If the force input is a sine wave, the velocity equation for the coil is $v = V_m \text{Sin } wt$ where V_m is the maximum amplitude, and wt is $2\pi ft$. The frequency is f in cps, and t is in seconds. Referring to Figure 22 (a), the projection of point A on a vertical line, as the wheel rotates counterclockwise, represents simple harmonic motion, i.e., a sine wave as shown in Figure 22 (b).

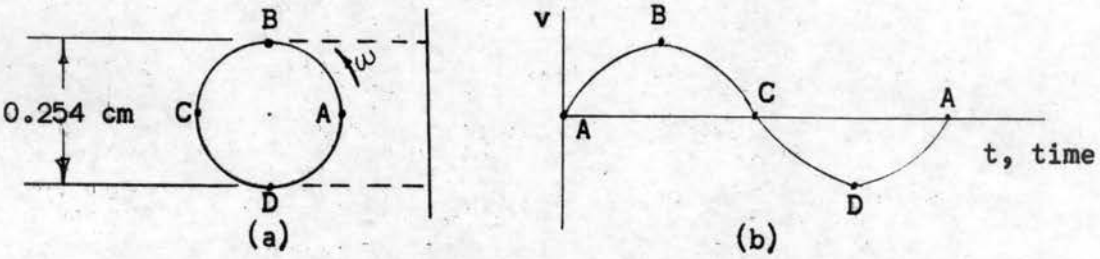

Figure 22. Projection of a point on the rim of a revolving wheel on a vertical line generates a sine wave.

The rim speed of the wheel is πD x RPS cm/sec = π x 0.254 RPS = 0.798 RPS cm/sec where RPS is revolutions per second (or cycles per second). For 100 cps, $V_m = 0.798 \times 100 = 79.8$ cm/sec., and $e = BL79.8\text{Sin}628t\ 10^{-8}$ volts. For B = 4800 gausses, and L = 915 cm, $e = 4800 \times 915 \times 79.8\text{Sin}628t$

10^{-8} = 3.505Sin628t volts. The 3.505 is the maximum value of the generated voltage. In texts on Alternating Current Circuits, it is shown that the RMS (root-mean-square) or effective value with respect to heating is E_{max} x 0.707 = 3.505 x 0.707 = 2.475 RMS volts. This is the value indicated on a.c. voltmeters, and the value used in calculating current and power. With the coil ends shorted, the theoretical short-circuit current would be E/R = 2.475/3.55 = 0.697 amperes. E and I_{sc} will vary directly with frequency.

At 200 cps: E = 2.475 x 2 = 4.95^{V}, and I_{sc} = 0.697 x 2 = 1.394^{A}
400 cps: E = 9.9^{V} I_{sc} = 2.788^{A}
1000 cps: E = 15.1^{V} I_{sc} = 6.97^{A}

The coil need not be operated under short-circuit conditions in which case the current will be generated voltage divided by the sum of the generator and load impedances (vector addition).

Since v = V_mSin wt was assumed for velocity, displacement x equals $\int V_m$Sin wt = $-V_m/w$ Cos wt, and acceleration a = dv/dt = wV_mCos wt. These relationships are depicted in Figure 23. The velocity is a maximum as the coil goes through the midposition where acceleration and displacement are zero.

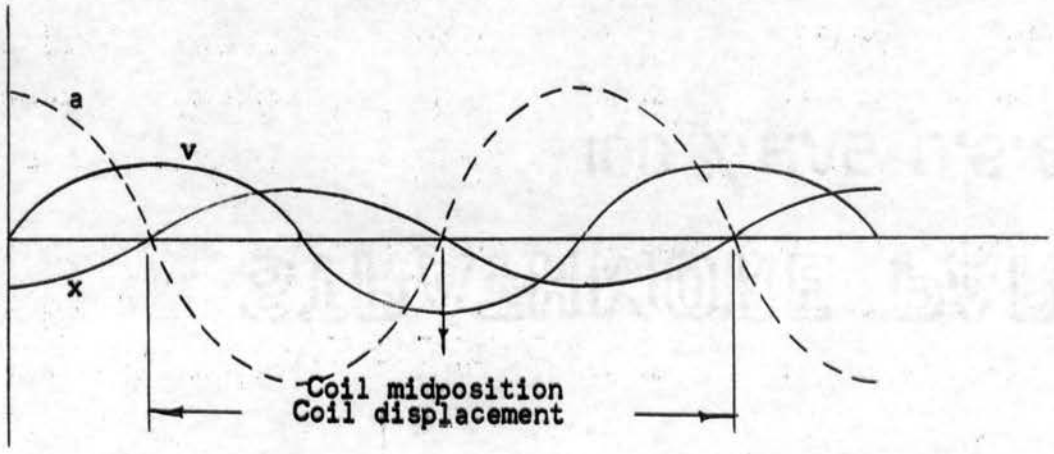

Figure 23. Relationship of displacement, x, velocity, v, and acceleration, a.

The weight of the coil assembly was 9 grams or 0.0199 pounds. It was convenient to make calculations in the British gravitational system.

100 cps

V_m = 79.8 cm/sec or 2.62 ft/sec.

$w = 2\pi f = 6.28 \times 100 = 628$ radians/sec.

$a = wV_m \cos wt$ which is a maximum when Cos wt = 1

$= 628 \times 2.62 = 1645$ ft/sec^2

$a/32.2 = 1645/32.2 = 51.1$ g's. (31)

$F = W/g\ (a) = 0.0199/32.2 \times 1645 = 0.000618 \times 1645 = 1.018$ lbs. (32)

200 cps

$V_m = 5.24$ ft/sec; $w = 1256$ rad/sec; $a = 1256 \times 5.24 = 6580$ ft/sec.^{2}

$a/32.2 = 6580/32.2 = 204$ g's.

$F = W/g\ (a) = 0.000618 \times 6580 = 4.07$ pounds.

1000 cps

$V_m = 26.2$ ft/sec; $w = 6280$ rad/sec; $a = 164{,}500$ ft/sec.^{2}

$164{,}500/32.2 = 5110$ g's; $F = 0.000618 \times 164{,}500 = 101.8$ pounds.

These calculations were for the coil assembly weight alone. The weight of the drive rod and associated moving elements would have to be added as would the electrical load and losses. At 1000 cps the acceleration becomes formidable, and may be unobtainable before coil frame or other parts fail.

The magnitude of the force acting on the coil due to motor action when current flows is $F = BLI_{ab}$ or $F = 0.1BLI$ in the CGS system from equation (9).

Dynes $\times 2.248 \times 10^{-6}$ = pounds.

$$\text{Lbs} = \frac{\text{Dynes} \times 2.248}{10^6} = \frac{0.1BLI \times 2.248}{10^6} = 0.2248BLI10^{-6} \text{ pounds,} \quad (33)$$

using B in gausses and L in centimeters. This assumes that the velocity input is sinusoidal so that the generated voltage will have the same wave shape.

Impedance, as commonly written in complex form, $Z = R \pm jX$, where R

is resistance and X is reactance in ohms, will be used.

$$F = 0.2248 \times 10^{-6}\ BLI = 0.2248 \times 10^{-6}\ BL\left(\frac{BLV_m \sin \omega t\ 10^{-8}}{Z/\theta}\right) \qquad (34)$$

$$= 0.2248 \times 10^{-14}\ B^2L^2\ \frac{V_m \sin (\omega t \not< 180^\circ - \theta)}{/Z/} \text{ pounds.}$$

The 180° is necessary to indicate that F is exactly opposite to the driving force, F_i. Assuming that the reactance is inductive, the impedance angle, θ, is negative in the numerator. This indicates that the motor action force will not be in direct opposition to the driving force by an amount equal to the impedance angle. If the total impedance in the generator coil and in the load is purely resistive, $\theta = 0$, and the two forces are opposite in sense.

$F = 0.2248 \times 10^{-6} \times 4800 \times 915\ I = 0.988\ I$, from equation (33).

100 cps ($R = 3.55$ ohms)
$F = 0.988 \times 3.505/3.55 = 0.975$ pounds (Max. as I_{max} was used).

200 cps
$F = 1.95$ pounds (maximum)

1000 cps
$F = 9.75$ pounds (maximum)

Plate III shows a photograph of the coil and coil frame.

Plate III

Coil and Coil Frame

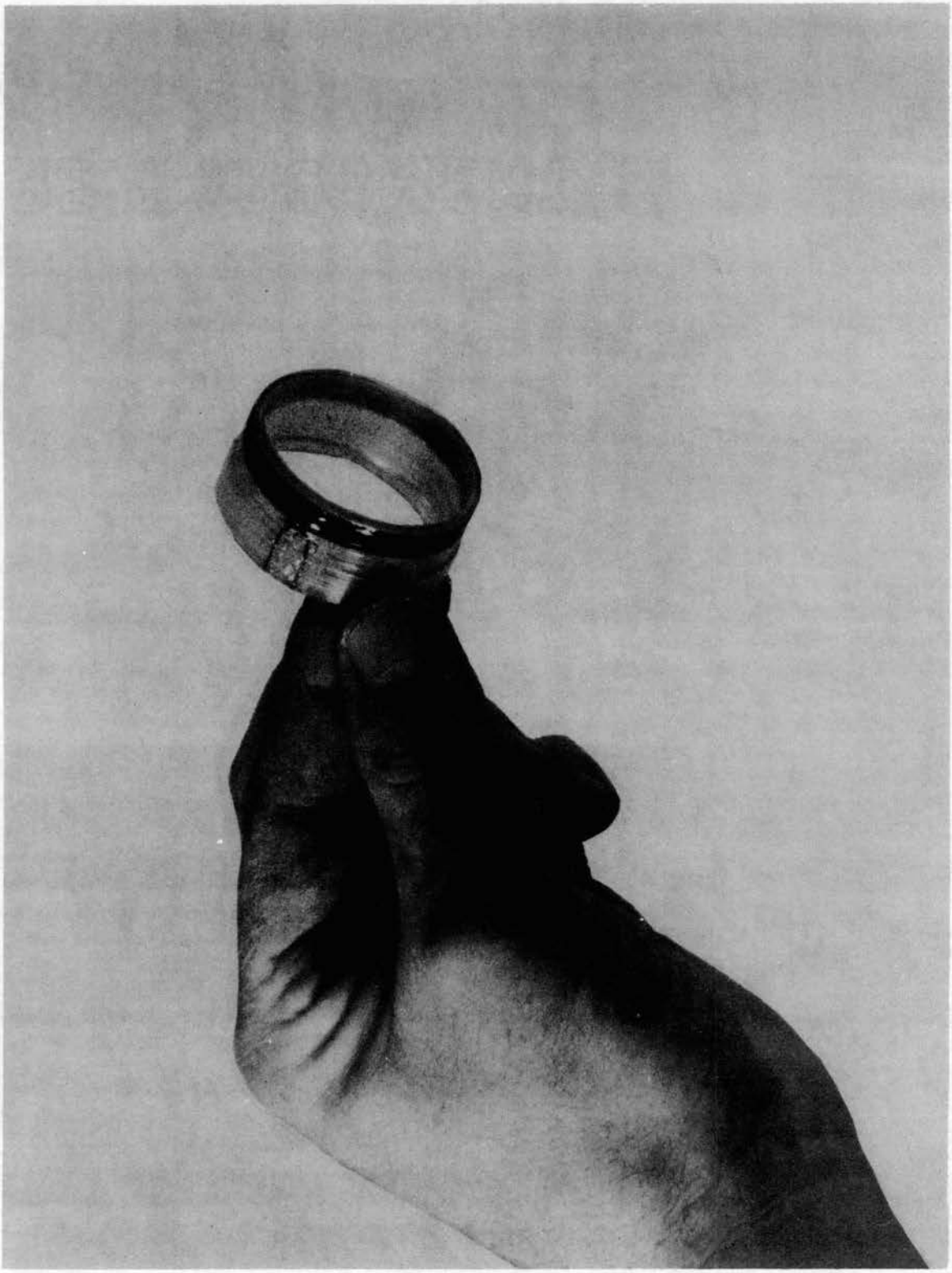

CHAPTER VII

DRIVING POWER SOURCE DESIGN

The source of mechanical driving power required to test the permanent-magnet generator constituted an auxiliary project that overshadowed the main object of this investigation. The upper frequency limit suggested by Air Force personnel was 1000 cps, which imposes several very severe problems in relation to the design of a suitable shaker. There are, in general, two types of shakers that could be considered for this type of application, namely, the electrodynamic shaker and the mechanical shaker.

An electrodynamic shaker[23] is a testing device for producting an alternating force that vibrates or shakes objects attached to its armature. The characteristics of this device are such that the magnitude, waveform, and frequency of the force produced can all be controlled over wide ranges, and permit direct measurement of mechanical force and power delivery. The acceleration that a shaker can produce, expressed in g units, is equal to the shaker force divided by the weight shaken, i.e., $a/g = F/W$. When resonant conditions are present, displacement of the shaken part can be increased by a factor of from 20 to 150 times that obtained by the direct action of the shaker force.

The electrodynamic shaker is similar to the oscillating generator.

---

[23]Robert C. Lewis, Applying Shakers for Product Vibration Analysis, Reprinted by the Calidyne Company from Product Engineering, November, 1950.

The difference is that an a.c. current is introduced into a coil in a magnetic field instead of an a.c. current being taken from a coil. This type of shaker is available commercially. However, as the frequency increases, the displacement decreases. It was considered desirable in this work to hold the displacement constant. The Chief Sales Engineer of the MB Manufacturing Company, while on the campus for a symposium, reported that the best that his machine could do would be one-twenty fifth of the requirement. The limiting factor was the weight of the moving coil assembly of 0.6 pounds. Construction of a shaker was initiated, but was not completed beyond the shaker frame with a d.c. exciting coil and a double-ended coil frame of synthane material. Further development of this power source may be indicated after test of a mechanical shaker.

The design of the mechanical shaker was performed by Professor L. J. Fila, a mechanical engineer. The following material is presented here as a matter of interest, and does not represent the work of the author of this thesis. The discussion is a paraphrasing of the material that appeared in the WADC Project Progress Report No. 11.[24]

A preliminary design of the mechanical portion of the apparatus was completed by Professor Fila, and the device was constructed by the Research and Development Laboratory of the Oklahoma Institute of Technology. The original plan was to be able to operate and test the oscillating generator up to 1000 cps with a spring-mass resonance in the vicinity of 400 cps. However, the present design was limited to a maximum of around 150 cps with a total displacement of 0.1 inches.

---

[24]Paul A. McCollum, Progress Report No. 11, UNCONVENTIONAL ELECTRICAL POWER SOURCES, Equipment Laboratory Contract No. AF 33(616)-2237, Project No. 6058, Task No. 60280, (Oklahoma A&M College, June 15, 1956), pp. 20-21.

A d.c. motor is belted through 7-inch and 1.5-inch pulleys to a 5/8-inch shaft in bearings. The shaft has an off-set section (plus balancing off-sets to reduce vibration) on which a scotch-yoke mechanism operates. Horizontal motion is transmitted through an arm riding in bearings to the coil of the generator. A photograph of this device, as part of the entire experimental setup, appears in Plate IV.

Further development will be made after test of the preliminary model. For frequencies higher than the 150 cps, problems arise that require further study. The stiff spring and the relatively large mass of the moving parts present difficulties that are serious enough to indicate that it may not be possible to devise a system which can operate at 1000 cps.

The theoretical analysis of the critical operating conditions has been completed for 1000 cps operation. At the 0.1-inch displacement selected, the moving parts have a maximum acceleration of 10,020 g's, where g is the acceleration under gravity. If a uniform aluminum bar of 7 inches in length undergoes this acceleration it would be subjected to a stress which exceeds its endurance limit. Since 7 inches is the estimated smallest length for satisfactory support and instrumentation, the amplitude evidently must be reduced. If the displacement were reduced to 0.05 inches the acceleration would still be very large at 5010 g's.

Simple harmonic motion (sine wave) is desirable for the sake of correlating the experimental results with theory. A slider crank mechanism only approximates harmonic motion when the connecting rod is very much longer than the crank radius. This could not be utilized because of the size limitation. In addition, the slider crank has three joints, each of which requires some clearance between the joined parts. Clearance between the moving parts should be at a minimum. The slider

crank clearances combine to introduce possible motion comparable to the 0.05 inches displacement desired. In addition, impact loads on already highly stressed parts might cause failure.

The cam produces simple harmonic motion, and needs only one clearance. However, the cam has a serious bearing disadvantage. Allowable bearing stresses conflict with the requirement of small size. The cam depends on a line contact between the joined parts. In order to support the large dynamic loads of the moving parts under the highest acceleration, the length of the line contact should be 47.4 inches. A cam with an area contact is needed. Such a design is possible, but only at the expense of increasing the number of clearances to two.

The masses must be small to minimize the dynamic loads, and they must be large to keep the stresses below the endurance limit. Aluminum has the desired property of low density and is also nonmagnetic, but it does not have the high endurance limit of steel. Steel is necessary for its high bearing strength. If made of aluminum, the moving parts would weigh 0.4 pounds for a dynamic load of 2040 pounds. If the aluminum is replaced by steel, the weight would be 1.128 pounds, and the load 5740 pounds. A composite structure is necessary. The joining of the two materials should be accomplished without the use of threaded parts which normally have high stress concentration factors. Under dynamic conditions, the stress concentration factor can increase the nominal stresses by 290 per cent.

The spring also poses a mass-strength problem. Its elastic characteristic must combine with the mass of the moving parts to produce a frequency of 400 cps. This could be accomplished with a cantilever steel spring, 6 inches long, with a square section of 1.3 inches on the side.

This spring, however, adds 0.66 pounds to the moving masses, thereby raising the dynamic load to 5350 pounds. Also, to deflect the end of such a spring through 0.05 inches, requires a considerable force in itself.

The preceding remarks indicate that the development of a suitable shaker will require a considerable period of time. Although the oscillating generator may be improved with better materials and a coil of a larger diameter, the problem of shaking the coil at higher frequencies will be predominant.

Plate IV

Prime Mover and Permanent-Magnet Oscillating Generator

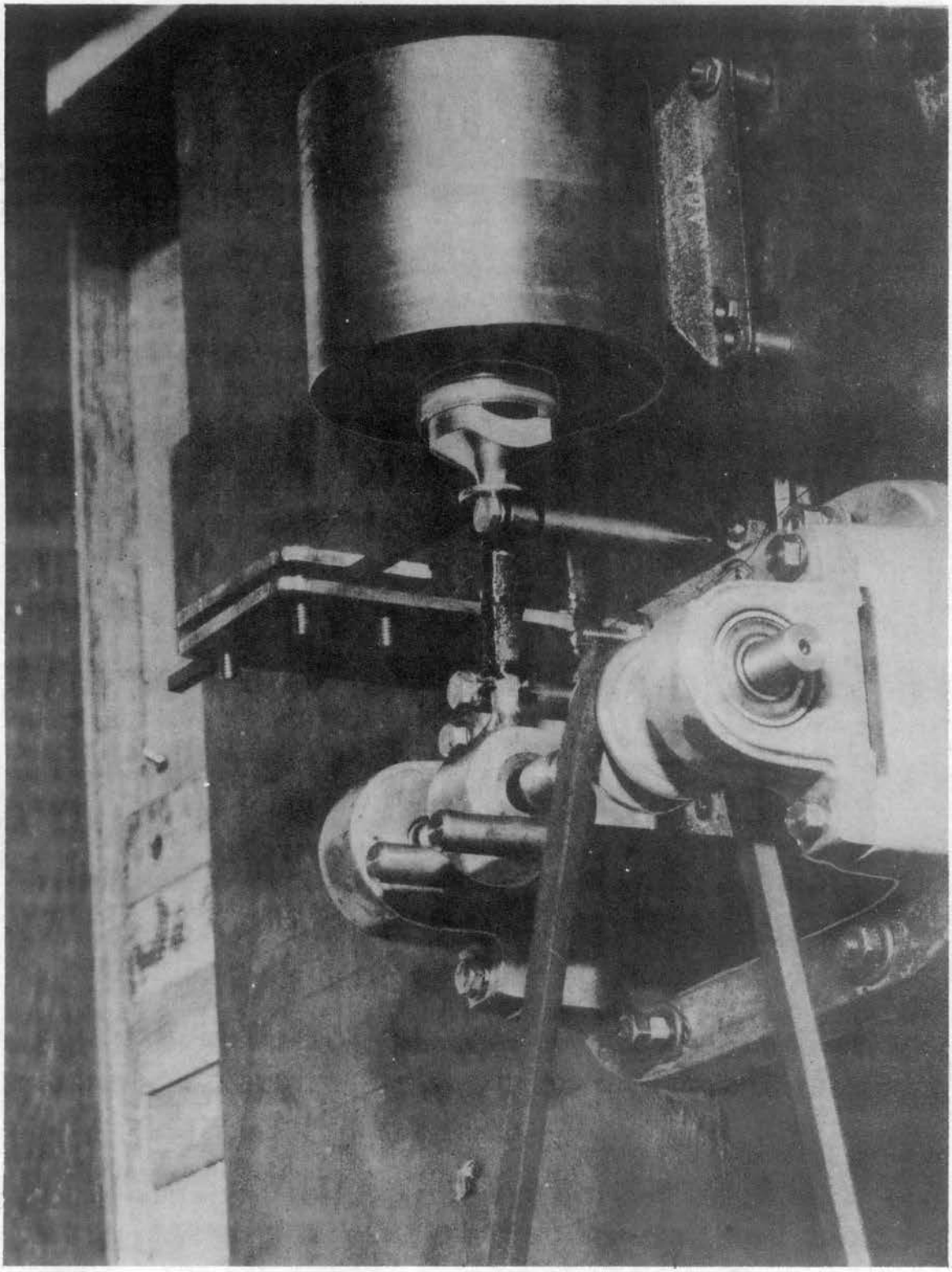

CHAPTER VIII

PERFORMANCE TESTS

Generator number two was magnetized to 5.1 kilogausses in the air gap, then demagnetized for magnet stabilization until the air gap flux density was 4.8 kilogausses. The permanent-magnet assembly was bolted to the 3/8-inch steel bedplate so that the coil was midway in the air gap. The relative position of the prime mover and generator is shown in Plate IV.

The following equipment was used in the performance tests:

1 a.c. amplifier, designed and constructed by Mr. Ralph Fisher

1 Cathode-Ray Oscilloscope, Dual-Beam, Dumont, Type 322, No. 09X78

1 Decade resistance box, 1 to 10 ohms in 1-ohm steps

1 Mechanical shaker with d.c. motor drive, described in Chap. VII.

2 Strain gages, SR-4, type C-1, 500-ohm, 3.42 gage factor

1 Strobotac, General Radio, Type 631-B, No. 15496

1 Vacuum-tube voltmeter, Hewlett-Packard, Model 400A

The test frequencies used were 60, 80, and 100 cps. Data was not taken at a frequency of 120 cps because the voltage was unstable due to the bending or "whip" of the drive rod. Since further tests will be made, it was undesirable to test the machine to destruction by raising the speed. The speed of the d.c. motor was adjusted with resistance in the armature circuit, using the strobotac neon light on the cam shaft as a monitor.

At each of the frequencies mentioned, the voltage was measured at

open circuit and at various values of resistive load. The currents were calculated using E/R since a milliammeter possessed more resistance than was desirable in the lower resistance ranges. Maximum power output occurs when the load resistance is the same as the generator coil resistance. A milliammeter would introduce more resistance than the internal resistance of 3.55 ohms of the generator. The short-circuit current was also calculated as open-circuit voltage divided by the coil resistance. The load power was calculated from I^2R. The results of this portion of the tests are shown by means of graphs contained in Figures 24, 25, and 26.

The oscillographic wave shape of the output voltage of the generator was observed on the oscilloscope at 100 cps and at selected values of load. Polaroid camera photographs of the wave shape are shown in Plate V. Theoretically, the scotch-yoke mechanism produces a sine wave of motion. However, the shock of reversal of direction distorted the wave shape. Although the general shape permitted the use of a RMS voltmeter to measure voltage without significant error, the wave distortion probably would be excessive when analyzed for harmonic components. The wave shape was improved when a spring was used to resonate with the moving masses at 76 cps. The mechanism also ran much more smoothly. However, it was concluded that a mechanical shaker was not suitable as a power source at higher frequencies.

One of the more important characteristics of a generator is the efficiency. Two 500-ohm C-1 strain gages were attached to the coil drive rod. These were energized in series with a ballast resistor by means of dry-cell batteries. The strain in the rod alternately compresses and elongates the strain gage so that the resistance changes accordingly. The change in voltage across the strain gages was capacitively coupled through an a.c. amplifier to a cathode-ray oscilloscope. The alternating

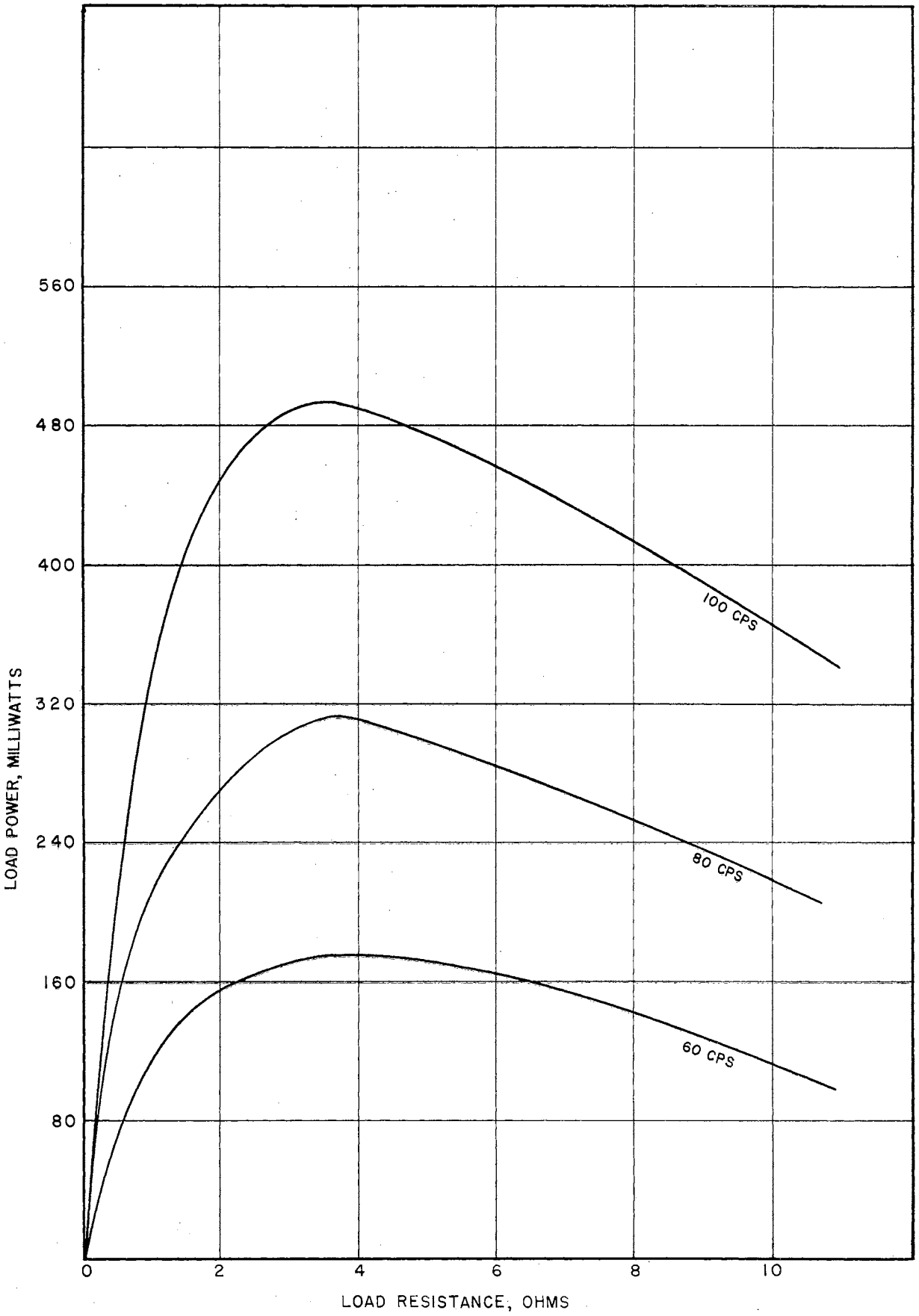

Figure 24. Generator Power Output

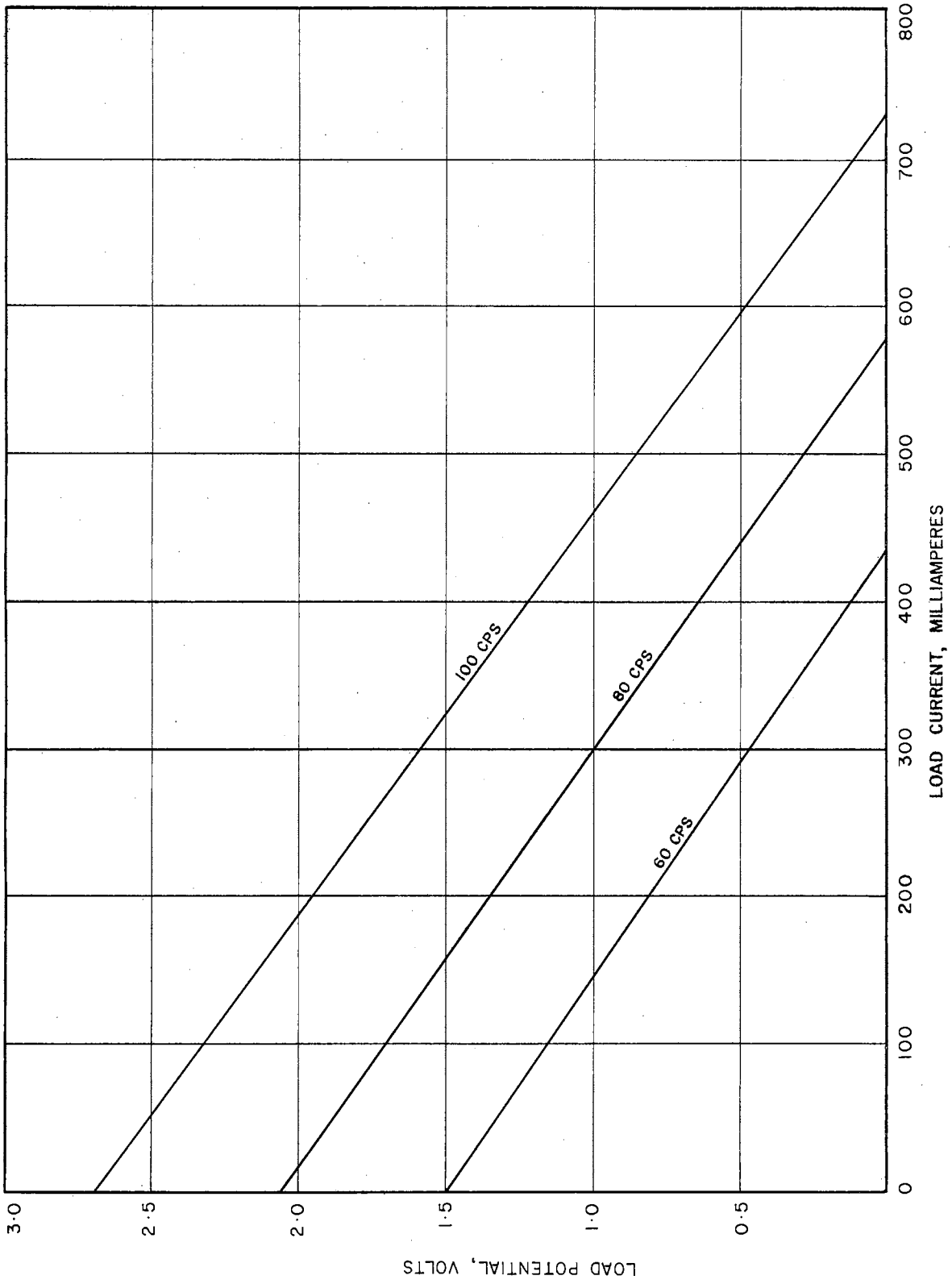

Figure 25. Variation of Load Voltage with Load Current

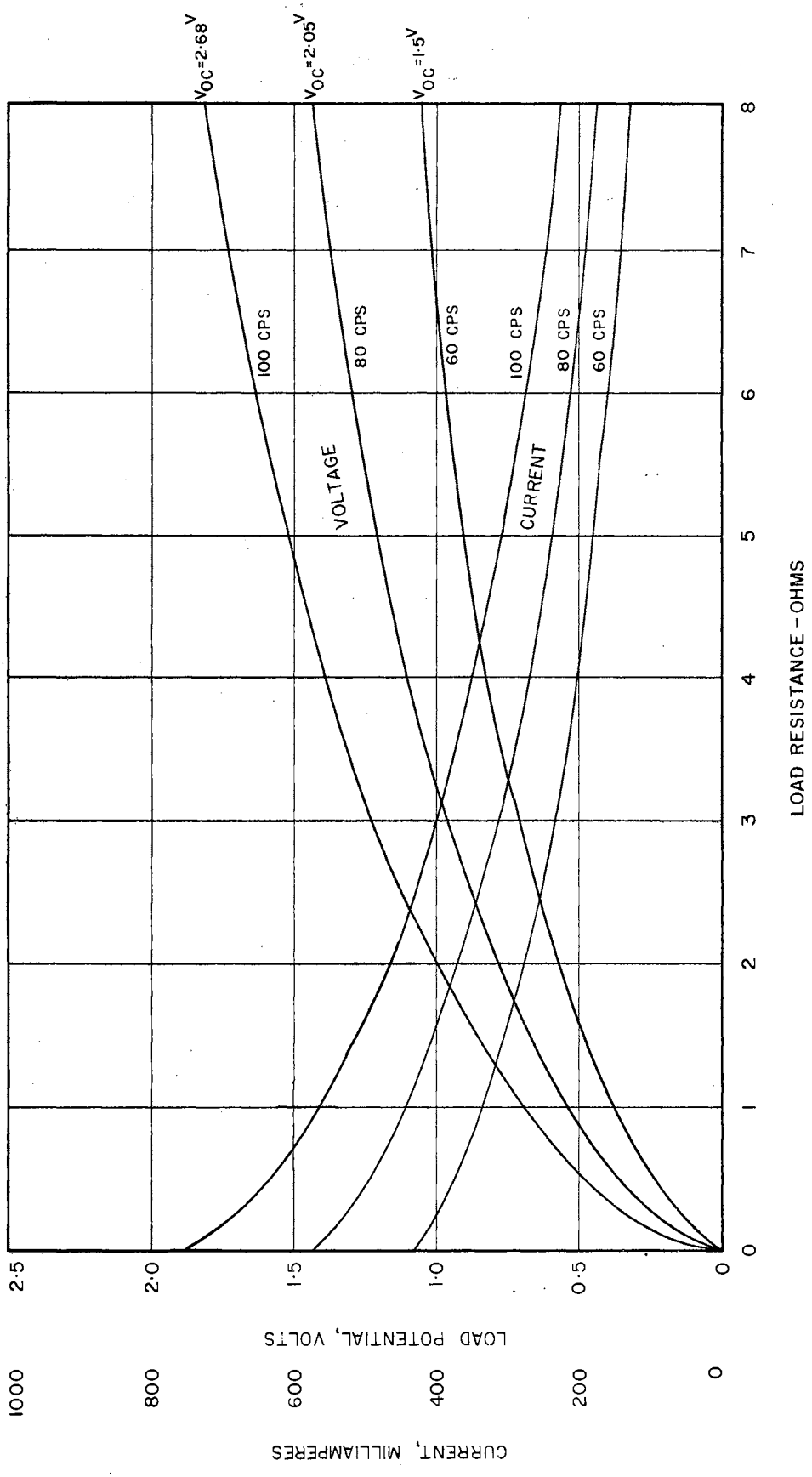

Figure 26. Variation of Load Current and Voltage with Load Resistance

Plate V

Oscillographic Photographs of Generator and Strain Gage Voltage

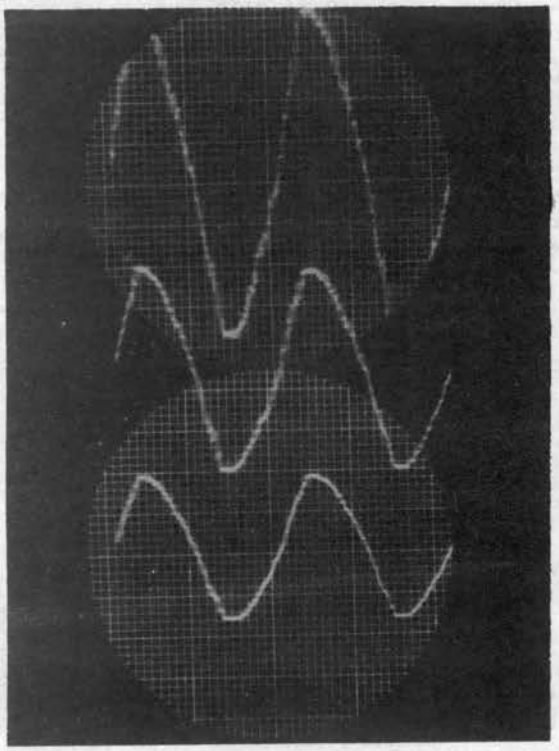

1. Generator voltage
   Upper: Open circuit
   Middle: Load of 6 ohms
   Lower: Load of 3 ohms

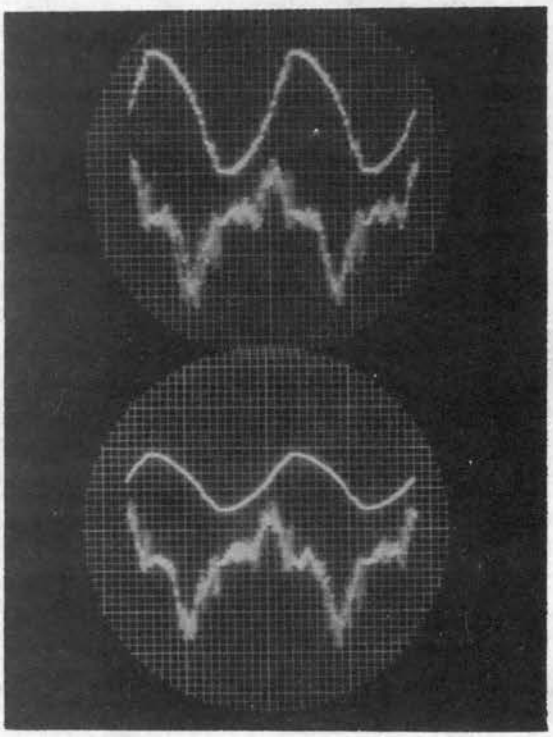

2. Generator voltage and strain gage voltage
   Upper: Open circuit
   Lower: Load of 3 ohms

pulsations would be a measure of the force applied to the coil frame. The voltage of the coil is in phase with the velocity of the drive rod. With the angle between the force input and the velocity from the oscilloscope, the power input would be $FvCos\theta$, where F is the force, v is the velocity, both in RMS values, and θ is the angle between the two quantities. The mechanical to electrical power conversion efficiency would then be the electrical power output divided by the power input, expressed in appropriate units. Unfortunately, the additional load on the drive rod due to added electrical load was so small as to be imperceptible on the oscilloscope. In other words, the inertia and shock loads were great when compared with the electrical load. Vibration also affected the output of the strain gages. A photograph of the strain gage output voltage is shown in Plate V.

It would appear that an electrodynamic shaker could be used to advantage since its power output can be found in terms of the current in the shaker coil, according to manufacturers of this equipment. However, this would be subject to experimental verification.

It may be seen from Figure 24 that maximum power occurs when the load resistance is the same as the resistance of the generator coil. The generator coil can be designed to match a particular load resistance. If the generated voltage is not as desired, then a compromise between coil resistance and generated voltage would be necessary.

Rated current has not been specified for the generator under test. Rated current would be governed by the allowable temperature rise, and this, in turn, would be limited by the type of insulation used. Due to the low voltages involved, there were no insulation voltage stress problems.

CHAPTER IX

ANALYSIS, SUMMARY, AND CONCLUSIONS

While reluctance formulas are valuable they must be multiplied by empirical factors in order to solve a magnetic circuit to predict the air gap flux. The design procedure to effect an optimum design, as developed in this thesis, proved successful to the extent that predicted air gap flux density was high by 4.76%. In view of the many variables, this was acceptable. Part of this error might be due to variance in permanent magnet properties from those given in the manufacturer's data, and part was undoubtedly due to the assist given to the MMF of the magnet by the small residual magnetism remaining in the iron portions of the circuit.

The inductance of an iron-clad electric circuit is usually high and variable. Due to the air gap used, however, this large inductance did not materialize. In fact, this property of the electric circuit was so small as to be practically unmeasurable. This was fortunate because the use of complex circuit parameters was avoided.

The calculated open-circuit RMS voltage at 100 cps was 2.475 volts as compared with the experimental value of 2.68 volts. Based on the calculated value, this difference represents an 8.28% error. A slightly greater stroke or flux density, and possibly a low-reading strobotac might account for this difference. In any event, a high value of voltage can be reduced by further demagnetization, whereas there is no remedy for a low voltage.

One disadvantage of the type of generator tested is there is no way in which voltage regulation improvement can be obtained. In this respect, it is similar to rotating permanent-magnet generators.

Oscillating motion presents serious problems not present in rotating equipment. A large mass cannot be shaken at a high frequency, and a small mass reduces the cross-sectional area of material so that insufficient strength remains. In addition, the shock of reversal results in a departure from the theoretical sine wave motion so desirable in electrical quantities. This non-sinusoidal motion results in distortion of the voltage wave shape.

The use of strain gages to provide a measure of the force input to the oscillating coil proved impractical (in this case) due to the fact that the electrical load was such a small part of the inertia and shock loads. In addition, the mechanical vibration had an undesirable effect upon the strain gage output. The failure of this part of the instrumentation prevented the finding of efficiency.

To summarize, it can be stated that an optimum design of a permanent-magnet generator was effected. Great difficulties were encountered in the dynamic testing of the device, centered in the lack of a suitable driving source and in instrumentation. Desired frequencies were not attained due to inherent problems connected with the motion of masses. Further development will increase the frequency range and methods of instrumentation, but the time factor prevents inclusion in this thesis.

The following conclusions and recommendations are made on the basis of observations and logic.

A permanent-magnet oscillating generator is not practical when a source of driving power must be provided. Such a generator would be

feasible when a driving source is provided by nature. For example, such a device might be mounted on an ocean buoy where the random motion due to the waves would be transmitted to a spring-mounted coil. The wave shape would be irregular, but such a wave could be rectified and used to charge batteries to operate, say, a transitorized radio. (The Army Signal Corps is developing a sound-powered radio transmitter which utilizes energy from a microphone in a sound power telephone handset.) The power input from the motion of ocean vessels or railroad cars would be free, but the weight of generators necessary to supply significant amounts of power might be prohibitive. The voltage and power output of the oscillating permanent-magnet generator can not be large so as to be comparable with that supplied by rotating equipment.

It was concluded that the mechanical shaker was unsuitable as a prime mover due to the shock of reversal, and due also to the large forces involved to obtain the large accelerations of mass at the higher frequencies desired. If further tests are desirable, it is recommended that the electro-dynamic shaker be considered.

Higher permeability materials might be used to obtain a larger flux density in the air gap. Also, if Alnico 5 could be heat treated in a radial magnetic field so that its directional quantities could be utilized in the face plate material, a great reduction in size and weight could be effected.

To avoid saturation in the pole piece at higher flux densities, the diameter of the pole piece must be increased. The diameter of the coil frame must also increase, allowing a greater length of wire to be wound thereon. This would increase the output voltage. However, a larger diameter permanent magnet would be required, which might not coincide with an optimum design for the least volume of magnetic material.

BIBLIOGRAPHY

Alnico Permanent Magnet Design Manual, Carboloy Department of General Electric Company, Detroit, 1955.

Alnico Permanent Magnets, General Magnetic Corporation, Detroit, n.d.

Applications Course, General Electric Company, Schenectady, 1947.

Barton, John, Jr. "An Oscillating Electric Generator." Unpublished Master's thesis, Oklahoma A&M College, Stillwater, 1955.

Bozorth, Richard M. Ferromagnetism, New York: D. Van Nostrand Company, Inc., 1951.

_____. "The Physics of Magnetic Materials," Electrical Engineering, Vol. 75, February, 1956, pp. 134-40.

Cioffi, P. P. "Stabilized Permanent Magnets," Transactions of the AIEE, Vol. 67, Part II, New York, 1948, pp. 1540-43.

Electrical Steel Sheets, Fourth Edition, United States Steel Corporation, Pittsburgh, 1955.

Hering, Carl. "An Imperfection in the Usual Statement of the Fundamental Law of Electromagnetic Induction," Proceedings of the American Institute of Electrical Engineers, Vol. 27, Part I, New York, 1908. p. 339.

Lewis, Robert C. Applying Shakers for Product Vibration Analysis, Reprinted by the Calidyne Company from Product Engineering, (November, 1950), New York: McGraw-Hill, 1950.

Magnetic Materials, Allegheny Ludlum Steel Corporation, Pittsburgh, 1947.

McCollum, Paul A. Progress Report No. 11, Unconventional Electrical Power Sources, Equipment Laboratory Contract No. AF 33(616)-2237, Project No. 6058, Task No. 60280, Oklahoma A&M College, June 15, 1956, pp. 20-21.

Permanent Magnets, Thomas & Skinner Steel Products Company, Inc., Indianapolis, 1955.

Proceedings of the American Institute of Electrical Engineers, Vol. 27, Part II, New York, 1908, pp. 1362-70.

Roters, Herbert C. Electromagnetic Devices, New York: John Wiley and Sons, 1941.

Spreadbury, F. G. Permanent Magnets, London: Pitman and Sons, Ltd., 1949.

Standard Definitions of Terms, with Symbols, Relating to Magnetic Testing, American Society for Testing Materials, ASTM Designation A340-49, Philadelphia, 1949.

Standard Methods of Test for Normal Induction and Hysteresis of Magnetic Materials, American Society for Testing Materials, Philadelphia, 1955.

Still, Alfred. Elements of Electrical Design, New York: McGraw-Hill, 1924.

Ward, Robert P. Introduction to Electrical Engineering, Second Edition, New York: Prentice-Hall, Inc., 1952.

VITA

Warren Estes Ray

Candidate for the Degree of

Master of Science

Thesis: PERMANENT-MAGNET OSCILLATING GENERATOR

Major Field: Electrical Engineering

Biographical:

Personal data: Born at Tuckerman, Arkansas, July 28, 1914

Education: Attended the city schools at Pryor, Oklahoma, graduating in April, 1933; after one semester in the evening division of Oklahoma City University in the Fall of 1941, graduated from the Oklahoma A&M College in May, 1952, with the degree of Bachelor of Science in Electrical Engineering.

Experience: Served in the U.S. Marine Corps from August, 1934, until retirement on January 1, 1948 (except for a period from September to December, 1940) with the rank of First Lieutenant; varied duties included that of adjutant, field artillery officer, and naval gunfire officer.

Employed by the General Electric Company on the Engineering Program from June, 1952, to September, 1953.

Employed by the School of Electrical Engineering, Oklahoma A&M College, as an instructor from September, 1953 to the end of January, 1956. Engaged on research from March 1 to July 31, 1956, under the leadership of Professor Paul A. McCollum, School of Electrical Engineering.

Professional Organizations: Associate Member, American Institute of Electrical Engineers; Registered Professional Engineer, State of Oklahoma.